Radiat Environ Biophys (2007) 46:311–325
DOI 10.1007/s00411-007-0120-5

ORIGINAL PAPER

DS02 fluence spectra for neutrons and gamma rays at Hiroshima and Nagasaki with fluence-to-kerma coefficients and transmission factors for sample measurements

Stephen D. Egbert · George D. Kerr · Harry M. Cullings

Received: 20 March 2007 / Accepted: 21 June 2007 / Published online: 21 July 2007

Abstract Fluence spectra at several ground distances in Hiroshima and Nagasaki are provided along with associated fluence-to-kerma coefficients from the Dosimetry System 2002 (DS02). Also included are transmission factors for calculating expected responses of in situ sample measurements of neutron activation products such as ^{32}P,^{36}Cl,^{39}Ar,^{41}Ca, ^{60}Co,^{63}Ni,^{152}Eu, and ^{154}Eu. The free-in-air (FIA) fluences calculated in 2002 are available for 240 angles, 69 energy groups, 101 ground distances, 5 heights, 4 radiation source components, 2 cities. The DS02 code uses these fluences partitioned to a prompt and delayed portion, collapsed to 58 energy groups and restricted to 97 ground distances. This is because the fluence spectra were required to be in the same format that was used in the older Dosimetry System 1986 (DS86) computer code, of which the DS02 computer code is a modification. The 2002 calculation fluences and the collapsed DS02 code fluences are presented and briefly discussed. A report on DS02, which is available on the website at the Radiation Effects Research Foundation, provides tables and figures of the A-bomb neutron and gamma-ray output used as the sources in the 2002 radiation transport calculations. While figures illustrating the fluence spectra at several ground ranges are presented in the DS02 Report, it does not include any tables of the calculated fluence spectra in the DS02 report. This paper provides, at several standard distances from the hypocenter, the numerical information which is required to translate the FIA neutron fluences given in DS02 to a neutron activation measurement or neutron and gamma-ray soft-tissue dose.

S. D. Egbert (✉)
Science Applications International Corporation,
MS A2, 10260 Campus Point Dr., San Diego, CA 92121, USA
e-mail: stephen.d.egbert@saic.com

G. D. Kerr
George D. Kerr Consulting, P.O. Box 12052,
Knoxville, TN 37912-0052, USA

H. M. Cullings
Radiation Effects Research Foundation, 5-2 Hijiyama Park,
Minami-ku, Hiroshima City 732-0815, Japan

Introduction

The cohort of the atomic bomb survivors of Hiroshima and Nagasaki comprises the major basis for investigations of late effects such as solid cancer and leukemia induced by ionizing radiation in humans. To deduce the corresponding risk coefficients, quantification of health effects and radiation doses are required. The recent DS02 Report on A-bomb survivor dosimetry describes calculations of neutron and gamma-ray fluences and the corresponding doses to survivors in both cities, and comparisons with measurements of activation and dose from the A-bombs [1]. While the required bomb parameters were determined from historical research, the leakage of neutrons and gamma rays from the bombs and the fission product neutron and gamma-ray emissions in the fireball were determined from new studies by staff members at the Los Alamos National Laboratory (LANL). The prompt radiation transport from the bomb to the ground was calculated at Oak Ridge National Laboratory (ORNL) and the delayed radiation transport from the fireball to the ground was calculated at Science Applications International Corporation (SAIC). Radiation transport in an air-over-ground environment is generally calculated using either discrete ordinates or Monte Carlo methods [2]. Both methods were used in this work. However, only the discrete ordinates transport (DOT) calculations are currently capable of providing sufficiently detailed energy and

angular distributions of the air-transported radiation fields at every 25 m out to the large distances (2,500 m) of interest in the dosimetry for the atomic bomb survivors at Hiroshima and Nagasaki [1, 2].

The resulting free-in-air (FIA) radiation fluences near the ground were saved, combined, and used for several tasks related to the calculation and verification of a survivors' radiation dose. For example, the FIA radiation fluences were transported into rocks, roof tiles, bricks, and other objects using Monte Carlo computer codes and then folded with various radiation responses to compare with the hundreds of in situ sample measurements made by US, Japanese, and German scientists. These efforts included thermal luminescence dosimetry (TLD) measurements in quartz crystals from gamma rays as well as neutron activation measurements of ^{60}Co (5.271 years), ^{152}Eu (13.51 years), ^{154}Eu (8.59 years), ^{36}Cl (301,000 years), and ^{41}Ca (102,000 years) which had been produced by moderated A-bomb neutrons, and of ^{32}P (14.26 days), ^{63}Ni (100.1 years) and ^{39}Ar (269 years) which had been produced by fast A-bomb neutrons [3]. While these activation measurements had been made immediately after the bombing and continued during the following decades [4], they intensified during the development of the DS02 dosimetry system. Thus, newer measurement results became available recently dealing with the detection of ^{36}Cl in granite and concrete samples [5–8], of ^{152}Eu in granite samples [9–11], of ^{63}Ni in copper samples [12–14], and of ^{39}Ar in granite samples [15].

In addition, the calculated FIA radiation fluences were also transported through shielding materials and the human body to obtain organ-dose estimates for individual survivors using the DS02 computer code at Radiation Effects Research Foundation (RERF).

This paper provides a description of the FIA fluence data that was calculated during the DS02 work and gives a few tables of the DS02 fluence spectra at 1 m above ground and several representative distances from the hypocenters of the bombs at both cities. Additionally, fluence-to-kerma coefficients and transmission factors used in DS02 are provided to make them generally available for calculating kerma and responses for future sample measurements at the two cities.

Materials and methods

2002 Calculation energy group boundaries and fluence-to-kerma coefficients

In 2002 the radiation calculations were carried out in a variety of energy group structures depending on the source resolution and the requirements of the calculation [1]. For example, the prompt radiation was calculated using the Vitamin-B6 (199 neutron/42 gamma-ray) energy groups [16] to capture the fine spectral variations seen as the neutrons and gamma-rays leaked out through the bomb casings. There was also a concern that the thermal neutron fluence could be affected by thermal up-scatter near the air-ground interface and the Vitamin-B6 group cross section set allowed for up-scatter to be included in the calculation. The delayed radiation was generally calculated in the DABL69 (46 neutron/23 gamma-ray) energy groups [17], because the delayed source spectra were much smoother; it had been found that the thermal neutron up-scatter used for the prompt radiation was not critically important; and the delayed neutron doses were smaller. The fluence spectra for both prompt and delayed radiations were collapsed into the common energy group structure of DABL69 in Table 1.

Many methods, parameters and data used in the 2002 calculations represent significant improvements over those used in the DS86 calculations [18]. These included the energy spectra of all sources of neutrons and gamma rays, the Hiroshima yield and height of burst, and the angular distributions of the prompt radiation leakage from the Hiroshima bomb. For radiation transport, there were improvements in energy resolution, spatial meshing, cross sections, delayed-radiation transport code and time resolution of the density in the developing fireball. These changes resulted in better agreement between the 2002 calculations and measurements of neutron activation and gamma-ray dose than were obtained with calculations within the framework of DS86 [1]. The calculated fluences or doses at the two cities did not change drastically (i.e., the fluences at all ranges, energy groups, and cities changed by less than 25%) and most of the total doses changed by less than 10%. Thus, confidence was greatly increased in the fluence and dose calculations at all ranges for both cities. The 2002 calculations, which were the basis for the DS02 comparison with measurements and DS02 survivor dosimetry are more fully described in the DS02 Report, published in 2005 [1].

Fluence-to-kerma coefficients for soft tissue

Kerma is the sum of the initial energies of all charged particles liberated by indirectly ionizing radiations such as neutrons and photons in a small volume element of a specified material divided by the mass of the material in that volume element [19]. The DS02 fluence-to-kerma coefficients were based on the composition for total soft tissue of the body from ICRP-1975 Reference Man [20, 21], the energy mass-absorption coefficients for photons from Hubbell and Seltzer [22], and the elemental kerma coefficients for neutrons from ICRU Report 63 [23]. The kerma coefficients for photons are based on a soft-tissue composition composed of 12 elements. These 12 elements included the 11 most abundant elements in the body (H, C, N, O, Na, Mg, P, S, Cl, K

Table 1 Energy group boundaries and fluence-to-kerma coefficients for the 2002 calculations

Group no.	Upper energy boundary (MeV)	Soft-tissue kerma coefficient (Gy cm^2)
Neutron		
1	$1.96 \times 10^{+1}$	6.90×10^{-11}
2	$1.69 \times 10^{+1}$	6.73×10^{-11}
3	$1.45 \times 10^{+1}$	6.61×10^{-11}
4	$1.40 \times 10^{+1}$	6.57×10^{-11}
5	$1.38 \times 10^{+1}$	6.47×10^{-11}
6	$1.25 \times 10^{+1}$	6.38×10^{-11}
7	$1.22 \times 10^{+1}$	6.33×10^{-11}
8	$1.11 \times 10^{+1}$	6.04×10^{-11}
9	$1.00 \times 10^{+1}$	5.83×10^{-11}
10	$9.05 \times 10^{+0}$	5.54×10^{-11}
11	$8.19 \times 10^{+0}$	5.45×10^{-11}
12	$7.41 \times 10^{+0}$	5.12×10^{-11}
13	$6.38 \times 10^{+0}$	4.71×10^{-11}
14	$4.97 \times 10^{+0}$	4.58×10^{-11}
15	$4.72 \times 10^{+0}$	4.43×10^{-11}
16	$4.07 \times 10^{+0}$	4.18×10^{-11}
17	$3.01 \times 10^{+0}$	3.55×10^{-11}
18	$2.39 \times 10^{+0}$	3.33×10^{-11}
19	$2.05 \times 10^{+0}$	3.20×10^{-11}
20	$1.61 \times 10^{+0}$	2.89×10^{-11}
21	$1.26 \times 10^{+0}$	2.61×10^{-11}
22	$1.03 \times 10^{+0}$	2.50×10^{-11}
23	9.62×10^{-1}	2.22×10^{-11}
24	8.21×10^{-1}	2.06×10^{-11}
25	7.43×10^{-1}	1.93×10^{-11}
26	6.39×10^{-1}	1.79×10^{-11}
27	5.50×10^{-1}	1.63×10^{-11}
28	3.69×10^{-1}	1.29×10^{-11}
29	2.47×10^{-1}	1.02×10^{-11}
30	1.58×10^{-1}	8.06×10^{-12}
31	1.11×10^{-1}	5.64×10^{-12}
32	5.25×10^{-2}	3.57×10^{-12}
33	3.43×10^{-2}	2.61×10^{-12}
34	2.48×10^{-2}	2.14×10^{-12}
35	2.19×10^{-2}	1.49×10^{-12}
36	1.03×10^{-2}	6.39×10^{-13}
37	3.35×10^{-3}	2.21×10^{-13}
38	1.23×10^{-3}	9.25×10^{-14}
39	5.83×10^{-4}	4.49×10^{-14}
40	2.75×10^{-4}	2.09×10^{-14}
41	1.01×10^{-4}	1.04×10^{-14}
42	2.90×10^{-5}	9.37×10^{-15}
43	1.07×10^{-5}	1.36×10^{-14}
44	3.06×10^{-6}	2.28×10^{-14}
45	1.13×10^{-6}	3.74×10^{-14}
46	4.14×10^{-7}	1.50×10^{-13}
	1.00×10^{-11}	
Gamma ray		
47	$2.00 \times 10^{+1}$	3.78×10^{-11}
48	$1.40 \times 10^{+1}$	3.03×10^{-11}
49	$1.20 \times 10^{+1}$	2.66×10^{-11}
50	$1.00 \times 10^{+1}$	2.28×10^{-11}
51	$8.00 \times 10^{+0}$	1.98×10^{-11}
52	$7.00 \times 10^{+0}$	1.78×10^{-11}
53	$6.00 \times 10^{+0}$	1.61×10^{-11}
54	$5.00 \times 10^{+0}$	1.43×10^{-11}
55	$4.00 \times 10^{+0}$	1.21×10^{-11}
56	$3.00 \times 10^{+0}$	1.03×10^{-11}
57	$2.50 \times 10^{+0}$	8.96×10^{-12}
58	$2.00 \times 10^{+0}$	7.53×10^{-12}
59	$1.50 \times 10^{+0}$	5.84×10^{-12}
60	$1.00 \times 10^{+0}$	4.25×10^{-12}
61	7.00×10^{-1}	2.86×10^{-12}
62	4.50×10^{-1}	1.92×10^{-12}
63	3.00×10^{-1}	1.03×10^{-12}
64	1.50×10^{-1}	5.30×10^{-13}
65	1.00×10^{-1}	3.49×10^{-13}
66	7.00×10^{-2}	3.16×10^{-13}
67	4.50×10^{-2}	4.64×10^{-13}
68	3.00×10^{-2}	1.07×10^{-12}
69	2.00×10^{-2}	3.51×10^{-12}
	1.00×10^{-2}	

and Ca) plus iron (Fe) which is one of the most abundant elements in organs of special interest such as the lungs and red bone marrow [21]. The kerma coefficients for photons based on the energy mass-absorption from Hubbell and Seltzer span the energy range from 10 keV to 20 MeV.

The kerma coefficients for neutrons are based only on the four major elements of the body (H, C, N and O) with the mass fractions for the other eight elements (Na, Mg, P, S, Cl, K, Ca and Fe) being assigned to oxygen because the neutron kerma coefficients were not available for these eight elements in ICRP Report 63. This approach works well with the neutron energies of less than 20 MeV. At thermal energies, nearly all of the kerma in soft tissue comes from protons produced by neutron capture in nitrogen. At higher neutron energies between 1 keV and 1 MeV, the proton recoils from elastic scattering by hydrogen contribute 90% or more to the soft-tissue kerma. The recoil-proton contribution drops to about 80% at 10 MeV and 70% at 20 MeV, the highest neutron energy of interest here.

The remaining soft-tissue kerma is from heavier charged particles produced by a variety of nuclear reactions, primarily recoils of carbon, nitrogen, and oxygen atoms. The kerma coefficients in ICRU Report 63 are only provided down to 0.0253 eV, but the (n, p) cross section for nitrogen shows a 1/v dependence at thermal energies. Thus, it is possible to extrapolate the kerma coefficients to lower thermal energies of interest using 1/v scaling.

The DS02 fluence-to-kerma coefficients are discussed in more detail and compared with fluence-to-kerma coefficients from early studies in Chap. 12, Part A of the DS02 Report [1]. The DS02 kerma conversion coefficients are also provided in the DS02 Report in the multi-group formats of the DLC31 [24] and Vitamin-B6 Libraries [16], and in a point-wise format for use in the MCNP computer code [25].

Results

2002 Total fluence spectra at several ground ranges

The 2002 angular energy fluences were calculated with the discrete ordinates method, and results were saved from zero to 2,500 m ground range [ground range is the distance to the hypocenter, which is the vertical projection of the point of explosion (epicenter) to the ground] in 25 m increments and at five heights between 1 and 25 m. The fluence was obtained from the angular fluence by weighting each of the discrete angles. The 240 angular weights sum to one. The units for the fluence are particles cm^{-2}. The fluences were also collapsed into the coarser DABL69 energy group structure (Table 1). These fluences are given in Table 2 and 3 for Hiroshima and Nagasaki, respectively, at 1 m height above ground and for six ground ranges (0, 500, 1,000, 1,500, 2,000 and 2,500 m). The explosive yields and burst height are 16 kt (TNT) and 600 m for Hiroshima, and 21 kt and 503 m for Nagasaki, respectively. The kerma is calculated when the fluence distribution with respect to energy is folded with the fluence-to-kerma coefficients given in Table 1. These kerma values are within a percent of those found in Tables 11 and 13 on pages 186 and 192 of the DS02 Report. The kerma values in the DS02 Report were calculated using the original Vitamin-B6 fine group fluences and conversion coefficients. Collapsing fluence spectra to a coarser energy group structure usually causes a minor round off in the folded results.

2002 Total fluences and partial fluences for four bomb radiation sources

The 2002 total FIA fluences in Tables 2 and 3 are the sum of the partial fluences from calculations for each of the four bomb radiation sources. These are neutron and gamma-ray sources that are either prompt (fission and secondary emissions which leak through the bomb casing in less than approximately 10 μs) or delayed (emissions from the fission products distributed within the fireball in times greater than approximately 1 ms^{-1}). The four sources are commonly referred to as (1) prompt neutron bomb leakage, (2) delayed neutron fireball emission, (3) prompt gamma-ray bomb leakage, and (4) delayed gamma-ray fireball emission. Tables 4 and 5 give the fluences from each of these four sources at 1,500 m from the hypocenter in Hiroshima and Nagasaki, respectively. When the partial fluences are summed together the total fluences in the previous Tables 2 and 3 are obtained. The neutron and gamma-ray fluences are plotted as fluence per unit lethargy on a logarithmic energy scale at six standard ground ranges for Hiroshima and Nagasaki in Figs. 1, 2, 3, and 4. Only the neutron fluences above 0.01 MeV are plotted, because the neutron fluence per lethargy is nearly constant below 0.01 MeV and the thermal neutron Maxwellian peak is too narrow to be resolved with the lowest energy group. This also allows the energy structure of the dose-contributing fluence to be seen more clearly. The complete neutron and gamma-ray fluence spectra with fine energy resolution are shown on pp. 153–154 and 160–162 of the DS02 Report. The average value of the curve over any logarithmic range of energy, (E to 2.718 $\times$ E), corresponds to the neutron or gamma-ray fluence within that energy range. At distances greater than 1,000 m, which represent the majority of the survivor locations at the two cities, very little change is noted in either the spectral shape of the neutron or gamma-ray fluence with ground distance or distance from the hypocenter.

DS02 code fluences

The DS02 code, used at RERF to calculate survivor doses, is a modification of the DS86 code [18, 26]. The DS86 code was based on shielding calculations using the DLC31 (37 neutron/21 gamma-ray) group structure [24]. Because most of the shielding calculations in the DS86 code were reused in DS02, any new shielding calculations for DS02 were also collapsed into the DLC31 energy group structure. Therefore, the DS02 code FIA fluences used the same modified DLC31 (37 prompt neutron/21 prompt gamma-ray/21 delayed gamma-ray/lower 14 of 37 delayed neutron; i.e., group numbers 24–37) energy group structure of DS86.

The 2002 FIA fluences remained partitioned into prompt and delayed components to separate the survivors' prompt and delayed doses. This also permitted the code to perform a time-dependent shielding calculation if needed. The 2002 FIA secondary gamma-ray fluences produced from the prompt neutrons were added to the prompt gamma-ray

Table 2 Hiroshima 2002 total neutron and gamma-ray FIA fluences at 1 m above ground

Group no.	0 m (cm^{-2})	500 m (cm^{-2})	1,000 m (cm^{-2})	1,500 m (cm^{-2})	2,000 m (cm^{-2})	2,500 m (cm^{-2})
Neutron						
1	$0.00 \times 10^{+0}$	$0.00 \times 10^{+0}$	$0.00 \times 10^{+0}$	$0.00 \times 10^{+0}$	$0.00 \times 10^{+0}$	$0.00 \times 10^{+0}$
2	$6.20 \times 10^{+4}$	$8.45 \times 10^{+4}$	$1.65 \times 10^{+4}$	$6.56 \times 10^{+2}$	$3.20 \times 10^{+1}$	$1.33 \times 10^{+0}$
3	$4.30 \times 10^{+4}$	$6.53 \times 10^{+4}$	$1.53 \times 10^{+4}$	$1.04 \times 10^{+3}$	$5.65 \times 10^{+1}$	$2.56 \times 10^{+0}$
4	$5.58 \times 10^{+4}$	$2.41 \times 10^{+5}$	$1.35 \times 10^{+4}$	$7.81 \times 10^{+2}$	$3.95 \times 10^{+1}$	$1.91 \times 10^{+0}$
5	$7.18 \times 10^{+5}$	$6.74 \times 10^{+5}$	$1.01 \times 10^{+5}$	$5.14 \times 10^{+3}$	$2.80 \times 10^{+2}$	$1.33 \times 10^{+1}$
6	$3.33 \times 10^{+5}$	$2.67 \times 10^{+5}$	$4.35 \times 10^{+4}$	$2.46 \times 10^{+3}$	$1.18 \times 10^{+2}$	$5.56 \times 10^{+0}$
7	$3.73 \times 10^{+6}$	$2.74 \times 10^{+6}$	$3.00 \times 10^{+5}$	$1.80 \times 10^{+4}$	$9.71 \times 10^{+2}$	$4.48 \times 10^{+1}$
8	$1.01 \times 10^{+7}$	$8.25 \times 10^{+6}$	$7.75 \times 10^{+5}$	$5.19 \times 10^{+4}$	$2.49 \times 10^{+3}$	$1.25 \times 10^{+2}$
9	$3.01 \times 10^{+7}$	$1.77 \times 10^{+7}$	$2.34 \times 10^{+6}$	$1.60 \times 10^{+5}$	$9.51 \times 10^{+3}$	$5.58 \times 10^{+2}$
10	$1.24 \times 10^{+8}$	$4.18 \times 10^{+7}$	$5.20 \times 10^{+6}$	$3.77 \times 10^{+5}$	$2.59 \times 10^{+4}$	$1.65 \times 10^{+3}$
11	$8.88 \times 10^{+7}$	$4.96 \times 10^{+7}$	$5.09 \times 10^{+6}$	$3.39 \times 10^{+5}$	$2.03 \times 10^{+4}$	$1.27 \times 10^{+3}$
12	$3.54 \times 10^{+8}$	$1.89 \times 10^{+8}$	$2.22 \times 10^{+7}$	$1.68 \times 10^{+6}$	$1.10 \times 10^{+5}$	$7.06 \times 10^{+3}$
13	$1.75 \times 10^{+9}$	$7.39 \times 10^{+8}$	$7.39 \times 10^{+7}$	$4.91 \times 10^{+6}$	$3.09 \times 10^{+5}$	$1.97 \times 10^{+4}$
14	$8.68 \times 10^{+8}$	$3.77 \times 10^{+8}$	$4.36 \times 10^{+7}$	$3.39 \times 10^{+6}$	$2.58 \times 10^{+5}$	$1.80 \times 10^{+4}$
15	$1.82 \times 10^{+9}$	$6.65 \times 10^{+8}$	$6.26 \times 10^{+7}$	$4.17 \times 10^{+6}$	$2.77 \times 10^{+5}$	$1.86 \times 10^{+4}$
16	$4.35 \times 10^{+9}$	$1.31 \times 10^{+9}$	$9.77 \times 10^{+7}$	$5.54 \times 10^{+6}$	$3.33 \times 10^{+5}$	$2.16 \times 10^{+4}$
17	$1.03 \times 10^{+10}$	$3.27 \times 10^{+9}$	$2.46 \times 10^{+8}$	$1.27 \times 10^{+7}$	$6.63 \times 10^{+5}$	$3.74 \times 10^{+4}$
18	$2.69 \times 10^{+9}$	$9.29 \times 10^{+8}$	$7.71 \times 10^{+7}$	$4.14 \times 10^{+6}$	$2.28 \times 10^{+5}$	$1.26 \times 10^{+4}$
19	$1.99 \times 10^{+10}$	$5.85 \times 10^{+9}$	$4.14 \times 10^{+8}$	$2.08 \times 10^{+7}$	$1.03 \times 10^{+6}$	$5.53 \times 10^{+4}$
20	$2.60 \times 10^{+10}$	$6.65 \times 10^{+9}$	$4.08 \times 10^{+8}$	$1.90 \times 10^{+7}$	$9.05 \times 10^{+5}$	$4.77 \times 10^{+4}$
21	$4.42 \times 10^{+10}$	$1.04 \times 10^{+10}$	$5.66 \times 10^{+8}$	$2.37 \times 10^{+7}$	$1.07 \times 10^{+6}$	$5.51 \times 10^{+4}$
22	$2.21 \times 10^{+10}$	$4.85 \times 10^{+9}$	$2.45 \times 10^{+8}$	$9.95 \times 10^{+6}$	$4.45 \times 10^{+5}$	$2.29 \times 10^{+4}$
23	$6.18 \times 10^{+10}$	$1.34 \times 10^{+10}$	$6.21 \times 10^{+8}$	$2.19 \times 10^{+7}$	$8.98 \times 10^{+5}$	$4.42 \times 10^{+4}$
24	$5.40 \times 10^{+10}$	$1.12 \times 10^{+10}$	$4.92 \times 10^{+8}$	$1.69 \times 10^{+7}$	$6.73 \times 10^{+5}$	$3.28 \times 10^{+4}$
25	$7.91 \times 10^{+10}$	$1.59 \times 10^{+10}$	$6.65 \times 10^{+8}$	$2.22 \times 10^{+7}$	$8.73 \times 10^{+5}$	$4.20 \times 10^{+4}$
26	$1.33 \times 10^{+11}$	$2.68 \times 10^{+10}$	$1.04 \times 10^{+9}$	$3.17 \times 10^{+7}$	$1.14 \times 10^{+6}$	$5.27 \times 10^{+4}$
27	$2.67 \times 10^{+11}$	$5.07 \times 10^{+10}$	$1.86 \times 10^{+9}$	$5.44 \times 10^{+7}$	$1.97 \times 10^{+6}$	$8.96 \times 10^{+4}$
28	$3.18 \times 10^{+11}$	$5.77 \times 10^{+10}$	$2.00 \times 10^{+9}$	$5.59 \times 10^{+7}$	$1.98 \times 10^{+6}$	$8.95 \times 10^{+4}$
29	$4.07 \times 10^{+11}$	$6.97 \times 10^{+10}$	$2.27 \times 10^{+9}$	$6.15 \times 10^{+7}$	$2.11 \times 10^{+6}$	$9.36 \times 10^{+4}$
30	$3.23 \times 10^{+11}$	$5.35 \times 10^{+10}$	$1.66 \times 10^{+9}$	$4.37 \times 10^{+7}$	$1.48 \times 10^{+6}$	$6.51 \times 10^{+4}$
31	$6.64 \times 10^{+11}$	$1.06 \times 10^{+11}$	$3.16 \times 10^{+9}$	$8.14 \times 10^{+7}$	$2.73 \times 10^{+6}$	$1.18 \times 10^{+5}$
32	$3.53 \times 10^{+11}$	$5.52 \times 10^{+10}$	$1.59 \times 10^{+9}$	$4.04 \times 10^{+7}$	$1.34 \times 10^{+6}$	$5.76 \times 10^{+4}$
33	$2.58 \times 10^{+11}$	$4.00 \times 10^{+10}$	$1.14 \times 10^{+9}$	$2.87 \times 10^{+7}$	$9.51 \times 10^{+5}$	$4.09 \times 10^{+4}$
34	$9.67 \times 10^{+10}$	$1.50 \times 10^{+10}$	$4.22 \times 10^{+8}$	$1.06 \times 10^{+7}$	$3.48 \times 10^{+5}$	$1.50 \times 10^{+4}$
35	$5.44 \times 10^{+11}$	$8.38 \times 10^{+10}$	$2.34 \times 10^{+9}$	$5.81 \times 10^{+7}$	$1.91 \times 10^{+6}$	$8.18 \times 10^{+4}$
36	$8.52 \times 10^{+11}$	$1.30 \times 10^{+11}$	$3.55 \times 10^{+9}$	$8.73 \times 10^{+7}$	$2.85 \times 10^{+6}$	$1.22 \times 10^{+5}$
37	$7.84 \times 10^{+11}$	$1.18 \times 10^{+11}$	$3.17 \times 10^{+9}$	$7.68 \times 10^{+7}$	$2.47 \times 10^{+6}$	$1.05 \times 10^{+5}$
38	$6.20 \times 10^{+11}$	$9.28 \times 10^{+10}$	$2.44 \times 10^{+9}$	$5.86 \times 10^{+7}$	$1.87 \times 10^{+6}$	$7.88 \times 10^{+4}$
39	$6.55 \times 10^{+11}$	$9.75 \times 10^{+10}$	$2.53 \times 10^{+9}$	$6.02 \times 10^{+7}$	$1.90 \times 10^{+6}$	$7.95 \times 10^{+4}$
40	$9.32 \times 10^{+11}$	$1.38 \times 10^{+11}$	$3.53 \times 10^{+9}$	$8.28 \times 10^{+7}$	$2.60 \times 10^{+6}$	$1.08 \times 10^{+5}$
41	$1.26 \times 10^{+12}$	$1.83 \times 10^{+11}$	$4.63 \times 10^{+9}$	$1.08 \times 10^{+8}$	$3.35 \times 10^{+6}$	$1.38 \times 10^{+5}$
42	$1.08 \times 10^{+12}$	$1.56 \times 10^{+11}$	$3.86 \times 10^{+9}$	$8.88 \times 10^{+7}$	$2.74 \times 10^{+6}$	$1.13 \times 10^{+5}$
43	$1.44 \times 10^{+12}$	$2.06 \times 10^{+11}$	$4.99 \times 10^{+9}$	$1.14 \times 10^{+8}$	$3.48 \times 10^{+6}$	$1.43 \times 10^{+5}$
44	$1.22 \times 10^{+12}$	$1.75 \times 10^{+11}$	$4.16 \times 10^{+9}$	$9.41 \times 10^{+7}$	$2.85 \times 10^{+6}$	$1.17 \times 10^{+5}$
45	$1.31 \times 10^{+12}$	$1.87 \times 10^{+11}$	$4.39 \times 10^{+9}$	$9.83 \times 10^{+7}$	$2.96 \times 10^{+6}$	$1.21 \times 10^{+5}$
46	$9.05 \times 10^{+12}$	$1.33 \times 10^{+12}$	$3.21 \times 10^{+10}$	$7.32 \times 10^{+8}$	$2.26 \times 10^{+7}$	$9.36 \times 10^{+5}$
Total	$2.29 \times 10^{+13}$	$3.45 \times 10^{+12}$	$9.09 \times 10^{+10}$	$2.24 \times 10^{+9}$	$7.37 \times 10^{+7}$	$3.20 \times 10^{+6}$

Table 2 continued

Group no.	0 m (cm^{-2})	500 m (cm^{-2})	1,000 m (cm^{-2})	1,500 m (cm^{-2})	2,000 m (cm^{-2})	2,500 m (cm^{-2})
Gamma ray						
47	$9.41 \times 10^{+5}$	$4.76 \times 10^{+5}$	$1.12 \times 10^{+5}$	$1.98 \times 10^{+4}$	$5.18 \times 10^{+3}$	$9.68 \times 10^{+2}$
48	$1.18 \times 10^{+7}$	$5.21 \times 10^{+6}$	$1.10 \times 10^{+6}$	$1.84 \times 10^{+5}$	$4.38 \times 10^{+4}$	$8.10 \times 10^{+3}$
49	$8.51 \times 10^{+10}$	$3.09 \times 10^{+10}$	$5.07 \times 10^{+9}$	$8.84 \times 10^{+8}$	$1.78 \times 10^{+8}$	$3.91 \times 10^{+7}$
50	$5.10 \times 10^{+10}$	$1.81 \times 10^{+10}$	$2.98 \times 10^{+9}$	$5.68 \times 10^{+8}$	$1.20 \times 10^{+8}$	$2.70 \times 10^{+7}$
51	$1.46 \times 10^{+11}$	$3.74 \times 10^{+10}$	$4.32 \times 10^{+9}$	$7.05 \times 10^{+8}$	$1.34 \times 10^{+8}$	$2.75 \times 10^{+7}$
52	$1.72 \times 10^{+11}$	$4.93 \times 10^{+10}$	$6.37 \times 10^{+9}$	$9.70 \times 10^{+8}$	$1.73 \times 10^{+8}$	$3.39 \times 10^{+7}$
53	$5.37 \times 10^{+11}$	$1.69 \times 10^{+11}$	$2.20 \times 10^{+10}$	$3.10 \times 10^{+9}$	$4.92 \times 10^{+8}$	$8.57 \times 10^{+7}$
54	$4.41 \times 10^{+11}$	$1.36 \times 10^{+11}$	$1.98 \times 10^{+10}$	$3.11 \times 10^{+9}$	$5.21 \times 10^{+8}$	$9.25 \times 10^{+7}$
55	$8.84 \times 10^{+11}$	$2.85 \times 10^{+11}$	$3.99 \times 10^{+10}$	$5.59 \times 10^{+9}$	$8.33 \times 10^{+8}$	$1.33 \times 10^{+8}$
56	$6.58 \times 10^{+11}$	$2.19 \times 10^{+11}$	$2.99 \times 10^{+10}$	$3.88 \times 10^{+9}$	$5.46 \times 10^{+8}$	$8.16 \times 10^{+7}$
57	$1.47 \times 10^{+12}$	$3.61 \times 10^{+11}$	$3.84 \times 10^{+10}$	$4.61 \times 10^{+9}$	$6.24 \times 10^{+8}$	$9.16 \times 10^{+7}$
58	$1.24 \times 10^{+12}$	$3.82 \times 10^{+11}$	$4.83 \times 10^{+10}$	$5.72 \times 10^{+9}$	$7.44 \times 10^{+8}$	$1.06 \times 10^{+8}$
59	$1.90 \times 10^{+12}$	$5.89 \times 10^{+11}$	$7.08 \times 10^{+10}$	$7.81 \times 10^{+9}$	$9.65 \times 10^{+8}$	$1.35 \times 10^{+8}$
60	$1.96 \times 10^{+12}$	$5.95 \times 10^{+11}$	$6.50 \times 10^{+10}$	$6.73 \times 10^{+9}$	$8.11 \times 10^{+8}$	$1.13 \times 10^{+8}$
61	$3.23 \times 10^{+12}$	$9.52 \times 10^{+11}$	$9.71 \times 10^{+10}$	$1.01 \times 10^{+10}$	$1.26 \times 10^{+9}$	$1.83 \times 10^{+8}$
62	$3.53 \times 10^{+12}$	$9.89 \times 10^{+11}$	$9.64 \times 10^{+10}$	$9.71 \times 10^{+9}$	$1.19 \times 10^{+9}$	$1.70 \times 10^{+8}$
63	$9.09 \times 10^{+12}$	$2.52 \times 10^{+12}$	$2.39 \times 10^{+11}$	$2.38 \times 10^{+10}$	$2.87 \times 10^{+9}$	$4.09 \times 10^{+8}$
64	$7.40 \times 10^{+12}$	$2.04 \times 10^{+12}$	$1.90 \times 10^{+11}$	$1.85 \times 10^{+10}$	$2.22 \times 10^{+9}$	$3.14 \times 10^{+8}$
65	$9.70 \times 10^{+12}$	$2.69 \times 10^{+12}$	$2.43 \times 10^{+11}$	$2.28 \times 10^{+10}$	$2.66 \times 10^{+9}$	$3.71 \times 10^{+8}$
66	$9.85 \times 10^{+12}$	$2.79 \times 10^{+12}$	$2.47 \times 10^{+11}$	$2.24 \times 10^{+10}$	$2.56 \times 10^{+9}$	$3.52 \times 10^{+8}$
67	$1.69 \times 10^{+12}$	$4.87 \times 10^{+11}$	$4.36 \times 10^{+10}$	$4.04 \times 10^{+9}$	$4.78 \times 10^{+8}$	$6.83 \times 10^{+7}$
68	$6.43 \times 10^{+10}$	$1.86 \times 10^{+10}$	$1.66 \times 10^{+9}$	$1.54 \times 10^{+8}$	$1.82 \times 10^{+7}$	$2.60 \times 10^{+6}$
69	$3.65 \times 10^{+8}$	$1.02 \times 10^{+8}$	$8.89 \times 10^{+6}$	$8.30 \times 10^{+5}$	$1.00 \times 10^{+5}$	$1.46 \times 10^{+4}$
Total	$5.41 \times 10^{+13}$	$1.54 \times 10^{+13}$	$1.51 \times 10^{+12}$	$1.55 \times 10^{+11}$	$1.94 \times 10^{+10}$	$2.83 \times 10^{+9}$

fluences. The neutron and gamma-ray fluences were then collapsed into the energy group structure of DLC31. The same was done for the delayed fluences. The DS02 code energy group boundaries are provided in Table 6. Tables 7 and 8 provide the 2002 prompt and delayed FIA fluences at 1,500 m as used in the DS02 code for Hiroshima and Nagasaki, respectively. It is noted from Tables 7 and 8 that, in addition to the prompt radiation, both the delayed neutrons and gamma rays make a significant contribution to fluence and dose at Nagasaki, while only the delayed gamma rays make a significant contribution to fluence and dose at Hiroshima.

Ground and surface composition effects on fluence

The effect of free water content in several different interface materials on the FIA fluence was investigated using the MCNP radiation transport code [25] and the prompt-neutron source term for the Hiroshima bomb from the DS02 studies [1]. The ratios of various nuclear reactions, using the FIA fluence at 1 m above different interface materials, to the same reactions at 1 m above wet ground (30% moisture) are compared in Table 9. In damp ground, the moisture content was taken as 15%, and it is zero in the dry ground. The composition and density of dry ground were taken from [2], and the composition and density for concrete and granite were taken from [9]. The 50 cm thickness of the normally used wet ground in the DS02 calculations was simply replaced with 50 cm of the material of interest using the appropriate composition and density. The three (n, γ) neutron capture reactions are proportional to the thermal neutron fluence. The neutron kerma results primarily from neutrons with energies between 0.5 and 2 MeV, and the (n, p) reactions in copper and sulfur are due to neutrons with energies greater than their threshold reaction energies of approximately 2 and 3 MeV, respectively.

The ratios in Table 9 were obtained from the MCNP radiation transport calculations between ground ranges of 200–1,000 m where the MCNP results were accurate to within 5%. The result for damp ground (15% moisture) is not very different from the normally-used wet ground (maximum change of 6% for neutron kerma). Hence, the wet soil used in our DS02 calculations gives reliable neutron fluences over ground for the range of free water content that would be normally expected in the soils of either Hiroshima or Nagasaki. The other data for dry soil, concrete, and gran-

Table 3 Nagasaki 2002 total neutron and gamma-ray FIA fluences at 1 m above ground

Group no.	0 m (cm^{-2})	500 m (cm^{-2})	1,000 m (cm^{-2})	1,500 m (cm^{-2})	2,000 m (cm^{-2})	2,500 m (cm^{-2})
Neutron						
1	$4.36 \times 10^{+6}$	$8.53 \times 10^{+5}$	$5.03 \times 10^{+4}$	$2.52 \times 10^{+3}$	$1.40 \times 10^{+2}$	$7.47 \times 10^{+0}$
2	$7.67 \times 10^{+6}$	$1.50 \times 10^{+6}$	$8.58 \times 10^{+4}$	$4.47 \times 10^{+3}$	$2.63 \times 10^{+2}$	$1.51 \times 10^{+1}$
3	$7.61 \times 10^{+6}$	$1.42 \times 10^{+6}$	$7.08 \times 10^{+4}$	$3.17 \times 10^{+3}$	$1.60 \times 10^{+2}$	$8.49 \times 10^{+0}$
4	$4.23 \times 10^{+6}$	$8.24 \times 10^{+5}$	$4.16 \times 10^{+4}$	$1.96 \times 10^{+3}$	$9.58 \times 10^{+1}$	$5.28 \times 10^{+0}$
5	$1.74 \times 10^{+7}$	$3.39 \times 10^{+6}$	$1.78 \times 10^{+5}$	$8.73 \times 10^{+3}$	$4.46 \times 10^{+2}$	$2.34 \times 10^{+1}$
6	$6.61 \times 10^{+6}$	$1.28 \times 10^{+6}$	$6.20 \times 10^{+4}$	$2.88 \times 10^{+3}$	$1.37 \times 10^{+2}$	$7.11 \times 10^{+0}$
7	$5.88 \times 10^{+7}$	$1.09 \times 10^{+7}$	$5.28 \times 10^{+5}$	$2.28 \times 10^{+4}$	$1.02 \times 10^{+3}$	$5.09 \times 10^{+1}$
8	$1.06 \times 10^{+8}$	$2.03 \times 10^{+7}$	$1.04 \times 10^{+6}$	$4.74 \times 10^{+4}$	$2.25 \times 10^{+3}$	$1.15 \times 10^{+2}$
9	$2.47 \times 10^{+8}$	$5.00 \times 10^{+7}$	$2.87 \times 10^{+6}$	$1.46 \times 10^{+5}$	$8.00 \times 10^{+3}$	$4.66 \times 10^{+2}$
10	$4.97 \times 10^{+8}$	$1.02 \times 10^{+8}$	$6.55 \times 10^{+6}$	$3.62 \times 10^{+5}$	$2.22 \times 10^{+4}$	$1.36 \times 10^{+3}$
11	$5.53 \times 10^{+8}$	$1.05 \times 10^{+8}$	$5.98 \times 10^{+6}$	$3.07 \times 10^{+5}$	$1.69 \times 10^{+4}$	$1.01 \times 10^{+3}$
12	$2.06 \times 10^{+9}$	$4.13 \times 10^{+8}$	$2.69 \times 10^{+7}$	$1.51 \times 10^{+6}$	$8.95 \times 10^{+4}$	$5.76 \times 10^{+3}$
13	$7.38 \times 10^{+9}$	$1.42 \times 10^{+9}$	$8.73 \times 10^{+7}$	$4.61 \times 10^{+6}$	$2.59 \times 10^{+5}$	$1.58 \times 10^{+4}$
14	$3.18 \times 10^{+9}$	$6.83 \times 10^{+8}$	$5.18 \times 10^{+7}$	$3.23 \times 10^{+6}$	$2.17 \times 10^{+5}$	$1.53 \times 10^{+4}$
15	$6.22 \times 10^{+9}$	$1.17 \times 10^{+9}$	$6.83 \times 10^{+7}$	$3.78 \times 10^{+6}$	$2.27 \times 10^{+5}$	$1.49 \times 10^{+4}$
16	$1.17 \times 10^{+10}$	$2.00 \times 10^{+9}$	$9.81 \times 10^{+7}$	$4.84 \times 10^{+6}$	$2.73 \times 10^{+5}$	$1.74 \times 10^{+4}$
17	$2.03 \times 10^{+10}$	$3.79 \times 10^{+9}$	$1.99 \times 10^{+8}$	$9.14 \times 10^{+6}$	$4.75 \times 10^{+5}$	$2.77 \times 10^{+4}$
18	$4.94 \times 10^{+9}$	$9.76 \times 10^{+8}$	$5.67 \times 10^{+7}$	$2.75 \times 10^{+6}$	$1.46 \times 10^{+5}$	$8.35 \times 10^{+3}$
19	$3.11 \times 10^{+10}$	$5.77 \times 10^{+9}$	$2.95 \times 10^{+8}$	$1.34 \times 10^{+7}$	$6.74 \times 10^{+5}$	$3.72 \times 10^{+4}$
20	$3.49 \times 10^{+10}$	$5.92 \times 10^{+9}$	$2.72 \times 10^{+8}$	$1.19 \times 10^{+7}$	$5.84 \times 10^{+5}$	$3.22 \times 10^{+4}$
21	$4.78 \times 10^{+10}$	$7.85 \times 10^{+9}$	$3.40 \times 10^{+8}$	$1.42 \times 10^{+7}$	$6.72 \times 10^{+5}$	$3.64 \times 10^{+4}$
22	$2.28 \times 10^{+10}$	$3.46 \times 10^{+9}$	$1.43 \times 10^{+8}$	$5.89 \times 10^{+6}$	$2.77 \times 10^{+5}$	$1.49 \times 10^{+4}$
23	$4.72 \times 10^{+10}$	$7.64 \times 10^{+9}$	$3.07 \times 10^{+8}$	$1.20 \times 10^{+7}$	$5.41 \times 10^{+5}$	$2.84 \times 10^{+4}$
24	$3.67 \times 10^{+10}$	$5.89 \times 10^{+9}$	$2.33 \times 10^{+8}$	$8.97 \times 10^{+6}$	$4.01 \times 10^{+5}$	$2.07 \times 10^{+4}$
25	$5.01 \times 10^{+10}$	$7.85 \times 10^{+9}$	$3.05 \times 10^{+8}$	$1.15 \times 10^{+7}$	$5.09 \times 10^{+5}$	$2.63 \times 10^{+4}$
26	$6.50 \times 10^{+10}$	$1.06 \times 10^{+10}$	$4.14 \times 10^{+8}$	$1.51 \times 10^{+7}$	$6.48 \times 10^{+5}$	$3.33 \times 10^{+4}$
27	$1.18 \times 10^{+11}$	$1.85 \times 10^{+10}$	$7.06 \times 10^{+8}$	$2.56 \times 10^{+7}$	$1.09 \times 10^{+6}$	$5.55 \times 10^{+4}$
28	$1.33 \times 10^{+11}$	$1.95 \times 10^{+10}$	$7.19 \times 10^{+8}$	$2.58 \times 10^{+7}$	$1.09 \times 10^{+6}$	$5.48 \times 10^{+4}$
29	$1.48 \times 10^{+11}$	$2.14 \times 10^{+10}$	$7.66 \times 10^{+8}$	$2.70 \times 10^{+7}$	$1.12 \times 10^{+6}$	$5.63 \times 10^{+4}$
30	$1.06 \times 10^{+11}$	$1.54 \times 10^{+10}$	$5.40 \times 10^{+8}$	$1.89 \times 10^{+7}$	$7.78 \times 10^{+5}$	$3.90 \times 10^{+4}$
31	$1.94 \times 10^{+11}$	$2.86 \times 10^{+10}$	$9.94 \times 10^{+8}$	$3.43 \times 10^{+7}$	$1.41 \times 10^{+6}$	$7.01 \times 10^{+4}$
32	$9.37 \times 10^{+10}$	$1.41 \times 10^{+10}$	$4.86 \times 10^{+8}$	$1.67 \times 10^{+7}$	$6.84 \times 10^{+5}$	$3.39 \times 10^{+4}$
33	$6.65 \times 10^{+10}$	$1.01 \times 10^{+10}$	$3.47 \times 10^{+8}$	$1.19 \times 10^{+7}$	$4.86 \times 10^{+5}$	$2.40 \times 10^{+4}$
34	$2.44 \times 10^{+10}$	$3.73 \times 10^{+9}$	$1.28 \times 10^{+8}$	$4.38 \times 10^{+6}$	$1.79 \times 10^{+5}$	$8.84 \times 10^{+3}$
35	$1.33 \times 10^{+11}$	$2.04 \times 10^{+10}$	$7.00 \times 10^{+8}$	$2.39 \times 10^{+7}$	$9.83 \times 10^{+5}$	$4.84 \times 10^{+4}$
36	$1.96 \times 10^{+11}$	$3.05 \times 10^{+10}$	$1.04 \times 10^{+9}$	$3.56 \times 10^{+7}$	$1.46 \times 10^{+6}$	$7.15 \times 10^{+4}$
37	$1.67 \times 10^{+11}$	$2.65 \times 10^{+10}$	$9.04 \times 10^{+8}$	$3.06 \times 10^{+7}$	$1.25 \times 10^{+6}$	$6.15 \times 10^{+4}$
38	$1.25 \times 10^{+11}$	$2.01 \times 10^{+10}$	$6.87 \times 10^{+8}$	$2.32 \times 10^{+7}$	$9.45 \times 10^{+5}$	$4.67 \times 10^{+4}$
39	$1.26 \times 10^{+11}$	$2.05 \times 10^{+10}$	$7.00 \times 10^{+8}$	$2.36 \times 10^{+7}$	$9.60 \times 10^{+5}$	$4.72 \times 10^{+4}$
40	$1.69 \times 10^{+11}$	$2.81 \times 10^{+10}$	$9.55 \times 10^{+8}$	$3.21 \times 10^{+7}$	$1.30 \times 10^{+6}$	$6.35 \times 10^{+4}$
41	$2.15 \times 10^{+11}$	$3.62 \times 10^{+10}$	$1.23 \times 10^{+9}$	$4.10 \times 10^{+7}$	$1.65 \times 10^{+6}$	$8.04 \times 10^{+4}$
42	$1.83 \times 10^{+11}$	$2.97 \times 10^{+10}$	$1.01 \times 10^{+9}$	$3.34 \times 10^{+7}$	$1.34 \times 10^{+6}$	$6.50 \times 10^{+4}$
43	$2.75 \times 10^{+11}$	$3.78 \times 10^{+10}$	$1.29 \times 10^{+9}$	$4.25 \times 10^{+7}$	$1.72 \times 10^{+6}$	$8.27 \times 10^{+4}$
44	$2.98 \times 10^{+11}$	$3.13 \times 10^{+10}$	$1.05 \times 10^{+9}$	$3.48 \times 10^{+7}$	$1.41 \times 10^{+6}$	$6.78 \times 10^{+4}$
45	$4.14 \times 10^{+11}$	$3.33 \times 10^{+10}$	$1.09 \times 10^{+9}$	$3.60 \times 10^{+7}$	$1.45 \times 10^{+6}$	$7.04 \times 10^{+4}$
46	$3.99 \times 10^{+12}$	$2.74 \times 10^{+11}$	$8.48 \times 10^{+9}$	$2.81 \times 10^{+8}$	$1.13 \times 10^{+7}$	$5.52 \times 10^{+5}$
Total	$7.56 \times 10^{+12}$	$7.86 \times 10^{+11}$	$2.67 \times 10^{+10}$	$9.26 \times 10^{+8}$	$3.87 \times 10^{+7}$	$1.94 \times 10^{+6}$

Table 3 continued

Group no.	0 m (cm^{-2})	500 m (cm^{-2})	1,000 m (cm^{-2})	1,500 m (cm^{-2})	2,000 m (cm^{-2})	2,500 m (cm^{-2})
Gamma ray						
47	$1.18 \times 10^{+7}$	$3.96 \times 10^{+6}$	$7.40 \times 10^{+5}$	$1.47 \times 10^{+5}$	$3.41 \times 10^{+4}$	$9.01 \times 10^{+3}$
48	$2.77 \times 10^{+9}$	$9.09 \times 10^{+8}$	$1.58 \times 10^{+8}$	$3.02 \times 10^{+7}$	$6.59 \times 10^{+6}$	$1.59 \times 10^{+6}$
49	$2.34 \times 10^{+11}$	$6.64 \times 10^{+10}$	$1.02 \times 10^{+10}$	$1.69 \times 10^{+9}$	$3.45 \times 10^{+8}$	$8.12 \times 10^{+7}$
50	$1.79 \times 10^{+11}$	$5.29 \times 10^{+10}$	$8.52 \times 10^{+9}$	$1.49 \times 10^{+9}$	$3.06 \times 10^{+8}$	$6.98 \times 10^{+7}$
51	$2.46 \times 10^{+11}$	$5.93 \times 10^{+10}$	$8.21 \times 10^{+9}$	$1.29 \times 10^{+9}$	$2.46 \times 10^{+8}$	$5.27 \times 10^{+7}$
52	$3.78 \times 10^{+11}$	$9.58 \times 10^{+10}$	$1.30 \times 10^{+10}$	$1.93 \times 10^{+9}$	$3.46 \times 10^{+8}$	$6.97 \times 10^{+7}$
53	$1.27 \times 10^{+12}$	$3.24 \times 10^{+11}$	$4.03 \times 10^{+10}$	$5.37 \times 10^{+9}$	$8.50 \times 10^{+8}$	$1.51 \times 10^{+8}$
54	$1.09 \times 10^{+12}$	$3.10 \times 10^{+11}$	$4.23 \times 10^{+10}$	$5.97 \times 10^{+9}$	$9.52 \times 10^{+8}$	$1.63 \times 10^{+8}$
55	$2.30 \times 10^{+12}$	$6.50 \times 10^{+11}$	$8.18 \times 10^{+10}$	$1.03 \times 10^{+10}$	$1.47 \times 10^{+9}$	$2.25 \times 10^{+8}$
56	$2.16 \times 10^{+12}$	$5.89 \times 10^{+11}$	$6.67 \times 10^{+10}$	$7.53 \times 10^{+9}$	$9.71 \times 10^{+8}$	$1.39 \times 10^{+8}$
57	$2.66 \times 10^{+12}$	$6.85 \times 10^{+11}$	$7.75 \times 10^{+10}$	$8.62 \times 10^{+9}$	$1.10 \times 10^{+9}$	$1.54 \times 10^{+8}$
58	$3.39 \times 10^{+12}$	$8.95 \times 10^{+11}$	$9.93 \times 10^{+10}$	$1.06 \times 10^{+10}$	$1.30 \times 10^{+9}$	$1.80 \times 10^{+8}$
59	$5.73 \times 10^{+12}$	$1.48 \times 10^{+12}$	$1.46 \times 10^{+11}$	$1.44 \times 10^{+10}$	$1.69 \times 10^{+9}$	$2.30 \times 10^{+8}$
60	$5.83 \times 10^{+12}$	$1.49 \times 10^{+12}$	$1.32 \times 10^{+11}$	$1.23 \times 10^{+10}$	$1.40 \times 10^{+9}$	$1.93 \times 10^{+8}$
61	$9.89 \times 10^{+12}$	$2.40 \times 10^{+12}$	$1.96 \times 10^{+11}$	$1.83 \times 10^{+10}$	$2.20 \times 10^{+9}$	$3.16 \times 10^{+8}$
62	$1.10 \times 10^{+13}$	$2.49 \times 10^{+12}$	$1.94 \times 10^{+11}$	$1.77 \times 10^{+10}$	$2.07 \times 10^{+9}$	$2.92 \times 10^{+8}$
63	$2.84 \times 10^{+13}$	$6.29 \times 10^{+12}$	$4.77 \times 10^{+11}$	$4.28 \times 10^{+10}$	$4.98 \times 10^{+9}$	$6.97 \times 10^{+8}$
64	$2.34 \times 10^{+13}$	$5.11 \times 10^{+12}$	$3.77 \times 10^{+11}$	$3.32 \times 10^{+10}$	$3.82 \times 10^{+9}$	$5.33 \times 10^{+8}$
65	$2.92 \times 10^{+13}$	$6.52 \times 10^{+12}$	$4.65 \times 10^{+11}$	$3.94 \times 10^{+10}$	$4.41 \times 10^{+9}$	$6.02 \times 10^{+8}$
66	$2.83 \times 10^{+13}$	$6.58 \times 10^{+12}$	$4.59 \times 10^{+11}$	$3.76 \times 10^{+10}$	$4.12 \times 10^{+9}$	$5.58 \times 10^{+8}$
67	$5.40 \times 10^{+12}$	$1.24 \times 10^{+12}$	$8.62 \times 10^{+10}$	$7.23 \times 10^{+9}$	$8.20 \times 10^{+8}$	$1.15 \times 10^{+8}$
68	$2.09 \times 10^{+11}$	$4.76 \times 10^{+10}$	$3.30 \times 10^{+9}$	$2.76 \times 10^{+8}$	$3.15 \times 10^{+7}$	$4.42 \times 10^{+6}$
69	$1.15 \times 10^{+9}$	$2.56 \times 10^{+8}$	$1.78 \times 10^{+7}$	$1.51 \times 10^{+6}$	$1.74 \times 10^{+5}$	$2.49 \times 10^{+4}$
Total	$1.61 \times 10^{+14}$	$3.74 \times 10^{+13}$	$2.98 \times 10^{+12}$	$2.78 \times 10^{+11}$	$3.34 \times 10^{+10}$	$4.83 \times 10^{+9}$

ite suggests that the effects of the local neutron scattering environment can be very important when considering neutron activation of building materials or neutron kerma for shielded survivors.

Gamma-ray doses from the prompt and delayed gamma-ray bomb sources are unaffected by the moisture content of the ground. The ground moisture had some affect on secondary gamma rays produced by neutrons that interact with the ground. When the ground was recalculated using concrete, there was a 10% decrease in the secondary gamma-ray dose component directly under the Hiroshima burst, and no change beyond 1,000 m. For Nagasaki, there was almost no difference under the burst, but beyond 1,000 m this dose component increased by 10–15%. At Hiroshima, the drier concrete allows the bomb's primary neutron fluence (i.e., high energy neutrons) to penetrate and be captured deeper into its depth reducing the gamma-ray dose above the concrete because of the increased distance the gamma rays must travel back out to the surface. While this is also true at Nagasaki, there the drier concrete also reduces the neutron moderation of the bomb's primary fluence (i.e., low energy epithermal neutrons). The neutrons can scatter farther back up into the air; where they are eventually captured by nitrogen and emit a high energy gamma ray, which slightly increases the gamma-ray dose especially at far distances. These are negligible changes in the total (prompt, delayed and secondary) gamma-ray dose due to soil moisture content variations.

Transmission factors for measurement samples

Most measurement samples were chosen from shortly after the bombing until the present time so that their incident surface would be in the line-of-sight to the bomb. But there was always some sample material between the measured location and photon or neutron fluence incident on the surface of the sample. Also, the backscattering material had a composition which usually differed from the DS02 ground, and often neighboring structures provided varying amounts of side shielding. Customized shielding calculations, using the DS02 FIA fluence, were used to determine the activation or kerma at the measurement point for samples where the geometry and material were known. The ratio of the activation or kerma in the sample and that at 1 m above ground is called the transmission factor (TF). These calculated TFs were also used to estimate the shielding for other

Table 4 Hiroshima 2002 partial neutron and gamma-ray FIA fluences from four bomb radiation sources at 1 m above ground for a ground range of 1,500 m

Group no.	Prompt neutron (cm^{-2})	Delayed neutron (cm^{-2})	Prompt gamma (cm^{-2})	Delayed gamma (cm^{-2})
Neutron				
1	$0.00 \times 10^{+0}$	–	–	–
2	$6.56 \times 10^{+2}$	–	–	–
3	$1.04 \times 10^{+3}$	–	–	–
4	$7.81 \times 10^{+2}$	–	–	–
5	$5.14 \times 10^{+3}$	–	–	–
6	$2.46 \times 10^{+3}$	–	–	–
7	$1.80 \times 10^{+4}$	–	–	–
8	$5.19 \times 10^{+4}$	–	–	–
9	$1.60 \times 10^{+5}$	–	–	–
10	$3.77 \times 10^{+5}$	–	–	–
11	$3.39 \times 10^{+5}$	$2.78 \times 10^{+1}$	–	–
12	$1.68 \times 10^{+6}$	$2.78 \times 10^{+3}$	–	–
13	$4.88 \times 10^{+6}$	$2.81 \times 10^{+4}$	–	–
14	$3.36 \times 10^{+6}$	$3.36 \times 10^{+4}$	–	–
15	$4.13 \times 10^{+6}$	$3.85 \times 10^{+4}$	–	–
16	$5.48 \times 10^{+6}$	$6.10 \times 10^{+4}$	–	–
17	$1.24 \times 10^{+7}$	$3.04 \times 10^{+5}$	–	–
18	$4.00 \times 10^{+6}$	$1.36 \times 10^{+5}$	–	–
19	$2.01 \times 10^{+7}$	$6.83 \times 10^{+5}$	–	–
20	$1.83 \times 10^{+7}$	$6.58 \times 10^{+5}$	–	–
21	$2.27 \times 10^{+7}$	$9.45 \times 10^{+5}$	–	–
22	$9.54 \times 10^{+6}$	$4.02 \times 10^{+5}$	–	–
23	$2.08 \times 10^{+7}$	$1.11 \times 10^{+6}$	–	–
24	$1.60 \times 10^{+7}$	$8.96 \times 10^{+5}$	–	–
25	$2.10 \times 10^{+7}$	$1.22 \times 10^{+6}$	–	–
26	$2.98 \times 10^{+7}$	$1.91 \times 10^{+6}$	–	–
27	$5.11 \times 10^{+7}$	$3.37 \times 10^{+6}$	–	–
28	$5.22 \times 10^{+7}$	$3.62 \times 10^{+6}$	–	–
29	$5.75 \times 10^{+7}$	$4.07 \times 10^{+6}$	–	–
30	$4.07 \times 10^{+7}$	$2.96 \times 10^{+6}$	–	–
31	$7.59 \times 10^{+7}$	$5.55 \times 10^{+6}$	–	–
32	$3.77 \times 10^{+7}$	$2.77 \times 10^{+6}$	–	–
33	$2.68 \times 10^{+7}$	$1.97 \times 10^{+6}$	–	–
34	$9.83 \times 10^{+6}$	$7.30 \times 10^{+5}$	–	–
35	$5.41 \times 10^{+7}$	$4.01 \times 10^{+6}$	–	–
36	$8.12 \times 10^{+7}$	$6.04 \times 10^{+6}$	–	–
37	$7.14 \times 10^{+7}$	$5.32 \times 10^{+6}$	–	–
38	$5.45 \times 10^{+7}$	$4.07 \times 10^{+6}$	–	–
39	$5.61 \times 10^{+7}$	$4.19 \times 10^{+6}$	–	–
40	$7.70 \times 10^{+7}$	$5.79 \times 10^{+6}$	–	–
41	$9.99 \times 10^{+7}$	$7.56 \times 10^{+6}$	–	–
42	$8.26 \times 10^{+7}$	$6.28 \times 10^{+6}$	–	–
43	$1.06 \times 10^{+8}$	$8.02 \times 10^{+6}$	–	–
44	$8.75 \times 10^{+7}$	$6.55 \times 10^{+6}$	–	–
45	$9.16 \times 10^{+7}$	$6.76 \times 10^{+6}$	–	–
46	$6.79 \times 10^{+8}$	$5.23 \times 10^{+7}$	–	–
Gamma ray				
47	$1.97 \times 10^{+4}$	$1.58 \times 10^{+2}$	–	–
48	$1.74 \times 10^{+5}$	$9.13 \times 10^{+3}$	–	–
49	$8.61 \times 10^{+8}$	$2.16 \times 10^{+7}$	$1.45 \times 10^{+6}$	–
50	$4.96 \times 10^{+8}$	$1.25 \times 10^{+7}$	$4.52 \times 10^{+7}$	$1.37 \times 10^{+7}$
51	$5.23 \times 10^{+8}$	$1.32 \times 10^{+7}$	$1.13 \times 10^{+8}$	$5.65 \times 10^{+7}$
52	$7.90 \times 10^{+8}$	$2.02 \times 10^{+7}$	$5.35 \times 10^{+7}$	$1.06 \times 10^{+8}$
53	$2.29 \times 10^{+9}$	$6.20 \times 10^{+7}$	$6.74 \times 10^{+7}$	$6.75 \times 10^{+8}$
54	$1.45 \times 10^{+9}$	$3.95 \times 10^{+7}$	$7.76 \times 10^{+7}$	$1.54 \times 10^{+9}$
55	$1.70 \times 10^{+9}$	$4.68 \times 10^{+7}$	$1.06 \times 10^{+8}$	$3.73 \times 10^{+9}$
56	$8.70 \times 10^{+8}$	$2.39 \times 10^{+7}$	$6.21 \times 10^{+7}$	$2.93 \times 10^{+9}$
57	$1.06 \times 10^{+9}$	$3.20 \times 10^{+7}$	$7.67 \times 10^{+7}$	$3.44 \times 10^{+9}$
58	$1.24 \times 10^{+9}$	$3.59 \times 10^{+7}$	$8.74 \times 10^{+7}$	$4.36 \times 10^{+9}$
59	$1.60 \times 10^{+9}$	$4.61 \times 10^{+7}$	$1.19 \times 10^{+8}$	$6.05 \times 10^{+9}$
60	$1.39 \times 10^{+9}$	$3.99 \times 10^{+7}$	$1.03 \times 10^{+8}$	$5.20 \times 10^{+9}$
61	$2.55 \times 10^{+9}$	$7.24 \times 10^{+7}$	$1.75 \times 10^{+8}$	$7.26 \times 10^{+9}$
62	$2.31 \times 10^{+9}$	$6.68 \times 10^{+7}$	$1.62 \times 10^{+8}$	$7.18 \times 10^{+9}$
63	$5.38 \times 10^{+9}$	$1.58 \times 10^{+8}$	$3.84 \times 10^{+8}$	$1.78 \times 10^{+10}$
64	$4.22 \times 10^{+9}$	$1.21 \times 10^{+8}$	$3.04 \times 10^{+8}$	$1.38 \times 10^{+10}$
65	$4.57 \times 10^{+9}$	$1.22 \times 10^{+8}$	$3.41 \times 10^{+8}$	$1.78 \times 10^{+10}$
66	$4.37 \times 10^{+9}$	$9.06 \times 10^{+7}$	$3.44 \times 10^{+8}$	$1.76 \times 10^{+10}$
67	$1.11 \times 10^{+9}$	$1.03 \times 10^{+7}$	$9.17 \times 10^{+7}$	$2.83 \times 10^{+9}$
68	$4.28 \times 10^{+7}$	$2.43 \times 10^{+5}$	$3.65 \times 10^{+6}$	$1.07 \times 10^{+8}$
69	$2.61 \times 10^{+5}$	$8.32 \times 10^{+2}$	$2.17 \times 10^{+4}$	$5.47 \times 10^{+5}$

samples where few details were available on sample shielding. Chapters 7B, 8J, and 9E of the DS02 Report [1] thoroughly discuss the details of these calculated and estimated TFs for gamma rays, thermal neutrons and fast neutrons, respectively.

Transmission factors for TLD kerma from gamma rays range from 0.7 to 1.0 for samples in line-of-sight. The most important parameters affecting the TFs were incident angle to the surface and depth in the sample. An elevated sample increased the kerma by decreasing the slant range to the bomb. Some TLD samples had neighboring structures providing partial side shielding. Because of this partial shielding from buildings or trees, it was estimated that a few of the Nagasaki samples had an additional 20% reduction in kerma.

Transmission factors for thermal neutron activation samples ranged from 0.7 to 1.1 for samples within 10 cm of the irradiated surface. The most important parameter affecting TF was the hydrogen content. For samples that were deeper than 10 cm the TF dropped exponentially. At the deeper

Table 5 Nagasaki 2002 partial neutron and gamma-ray FIA fluences from four bomb radiation sources at 1 m above ground for a ground range of 1,500 m

Group no.	Prompt neutron (cm^{-2})	Delayed neutron (cm^{-2})	Prompt gamma (cm^{-2})	Delayed gamma (cm^{-2})
Neutron				
1	$2.52 \times 10^{+3}$	–	–	–
2	$4.47 \times 10^{+3}$	–	–	–
3	$3.17 \times 10^{+3}$	–	–	–
4	$1.96 \times 10^{+3}$	–	–	–
5	$8.73 \times 10^{+3}$	–	–	–
6	$2.88 \times 10^{+3}$	–	–	–
7	$2.28 \times 10^{+4}$	–	–	–
8	$4.74 \times 10^{+4}$	–	–	–
9	$1.46 \times 10^{+5}$	–	–	–
10	$3.62 \times 10^{+5}$	–	–	–
11	$3.07 \times 10^{+5}$	$7.91 \times 10^{+1}$	–	–
12	$1.50 \times 10^{+6}$	$7.50 \times 10^{+3}$	–	–
13	$4.54 \times 10^{+6}$	$7.39 \times 10^{+4}$	–	–
14	$3.15 \times 10^{+6}$	$8.36 \times 10^{+4}$	–	–
15	$3.68 \times 10^{+6}$	$9.52 \times 10^{+4}$	–	–
16	$4.69 \times 10^{+6}$	$1.46 \times 10^{+5}$	–	–
17	$8.57 \times 10^{+6}$	$5.72 \times 10^{+5}$	–	–
18	$2.52 \times 10^{+6}$	$2.29 \times 10^{+5}$	–	–
19	$1.22 \times 10^{+7}$	$1.14 \times 10^{+6}$	–	–
20	$1.08 \times 10^{+7}$	$1.07 \times 10^{+6}$	–	–
21	$1.28 \times 10^{+7}$	$1.47 \times 10^{+6}$	–	–
22	$5.27 \times 10^{+6}$	$6.24 \times 10^{+5}$	–	–
23	$1.04 \times 10^{+7}$	$1.64 \times 10^{+6}$	–	–
24	$7.65 \times 10^{+6}$	$1.31 \times 10^{+6}$	–	–
25	$9.74 \times 10^{+6}$	$1.77 \times 10^{+6}$	–	–
26	$1.24 \times 10^{+7}$	$2.72 \times 10^{+6}$	–	–
27	$2.09 \times 10^{+7}$	$4.74 \times 10^{+6}$	–	–
28	$2.07 \times 10^{+7}$	$5.04 \times 10^{+6}$	–	–
29	$2.14 \times 10^{+7}$	$5.59 \times 10^{+6}$	–	–
30	$1.48 \times 10^{+7}$	$4.05 \times 10^{+6}$	–	–
31	$2.67 \times 10^{+7}$	$7.60 \times 10^{+6}$	–	–
32	$1.29 \times 10^{+7}$	$3.77 \times 10^{+6}$	–	–
33	$9.19 \times 10^{+6}$	$2.70 \times 10^{+6}$	–	–
34	$3.38 \times 10^{+6}$	$9.98 \times 10^{+5}$	–	–
35	$1.85 \times 10^{+7}$	$5.49 \times 10^{+6}$	–	–
36	$2.74 \times 10^{+7}$	$8.24 \times 10^{+6}$	–	–
37	$2.35 \times 10^{+7}$	$7.19 \times 10^{+6}$	–	–
38	$1.77 \times 10^{+7}$	$5.51 \times 10^{+6}$	–	–
39	$1.79 \times 10^{+7}$	$5.67 \times 10^{+6}$	–	–
40	$2.43 \times 10^{+7}$	$7.83 \times 10^{+6}$	–	–
41	$3.08 \times 10^{+7}$	$1.02 \times 10^{+7}$	–	–
42	$2.49 \times 10^{+7}$	$8.47 \times 10^{+6}$	–	–
43	$3.17 \times 10^{+7}$	$1.08 \times 10^{+7}$	–	–
44	$2.60 \times 10^{+7}$	$8.81 \times 10^{+6}$	–	–
45	$2.69 \times 10^{+7}$	$9.10 \times 10^{+6}$	–	–
46	$2.09 \times 10^{+8}$	$7.14 \times 10^{+7}$	–	–
Gamma ray				
47	$1.50 \times 10^{+4}$	$3.12 \times 10^{+2}$	–	–
48	$5.73 \times 10^{+4}$	$1.08 \times 10^{+4}$	–	–
49	$1.59 \times 10^{+9}$	$2.47 \times 10^{+7}$	$7.81 \times 10^{+7}$	–
50	$9.37 \times 10^{+8}$	$1.43 \times 10^{+7}$	$5.29 \times 10^{+8}$	$1.24 \times 10^{+7}$
51	$9.52 \times 10^{+8}$	$1.60 \times 10^{+7}$	$2.60 \times 10^{+8}$	$6.67 \times 10^{+7}$
52	$1.42 \times 10^{+9}$	$2.40 \times 10^{+7}$	$3.66 \times 10^{+8}$	$1.25 \times 10^{+8}$
53	$4.03 \times 10^{+9}$	$7.27 \times 10^{+7}$	$4.67 \times 10^{+8}$	$8.00 \times 10^{+8}$
54	$2.63 \times 10^{+9}$	$4.58 \times 10^{+7}$	$1.46 \times 10^{+9}$	$1.84 \times 10^{+9}$
55	$2.99 \times 10^{+9}$	$5.42 \times 10^{+7}$	$1.90 \times 10^{+9}$	$5.34 \times 10^{+9}$
56	$1.55 \times 10^{+9}$	$2.77 \times 10^{+7}$	$1.46 \times 10^{+9}$	$4.50 \times 10^{+9}$
57	$1.83 \times 10^{+9}$	$3.86 \times 10^{+7}$	$1.51 \times 10^{+9}$	$5.25 \times 10^{+9}$
58	$2.14 \times 10^{+9}$	$4.23 \times 10^{+7}$	$1.79 \times 10^{+9}$	$6.65 \times 10^{+9}$
59	$2.79 \times 10^{+9}$	$5.44 \times 10^{+7}$	$2.37 \times 10^{+9}$	$9.15 \times 10^{+9}$
60	$2.41 \times 10^{+9}$	$4.70 \times 10^{+7}$	$2.02 \times 10^{+9}$	$7.84 \times 10^{+9}$
61	$4.42 \times 10^{+9}$	$8.53 \times 10^{+7}$	$2.98 \times 10^{+9}$	$1.09 \times 10^{+10}$
62	$3.98 \times 10^{+9}$	$7.90 \times 10^{+7}$	$2.88 \times 10^{+9}$	$1.08 \times 10^{+10}$
63	$9.24 \times 10^{+9}$	$1.85 \times 10^{+8}$	$6.80 \times 10^{+9}$	$2.66 \times 10^{+10}$
64	$7.15 \times 10^{+9}$	$1.39 \times 10^{+8}$	$5.40 \times 10^{+9}$	$2.05 \times 10^{+10}$
65	$7.46 \times 10^{+9}$	$1.34 \times 10^{+8}$	$5.99 \times 10^{+9}$	$2.58 \times 10^{+10}$
66	$6.86 \times 10^{+9}$	$9.30 \times 10^{+7}$	$5.94 \times 10^{+9}$	$2.47 \times 10^{+10}$
67	$1.72 \times 10^{+9}$	$1.01 \times 10^{+7}$	$1.57 \times 10^{+9}$	$3.92 \times 10^{+9}$
68	$6.66 \times 10^{+7}$	$2.33 \times 10^{+5}$	$6.27 \times 10^{+7}$	$1.47 \times 10^{+8}$
69	$3.97 \times 10^{+5}$	$9.46 \times 10^{+2}$	$3.69 \times 10^{+5}$	$7.41 \times 10^{+5}$

locations the important parameters were depth, hydrogen content, and the concentration of any neutron absorbing isotopes in the material, such as gadolinium.

Transmission factors for fast neutron activation copper reactions ranged from 0.8 to 1.1 and for sulfur reactions averaged about 0.93. These were all line-of-sight samples. The most important parameter was the amount of mass surrounding the sample, such as the thickness of the copper wire, the steel pipe containing the copper wire, or the porcelain insulators surrounding the sulfur. For example, the shielding of sulfur just due to the insulator was 0.85. The hydrogen content of the nearby building or street was also important. For example, a lower hydrogen content of concrete or dry soil increased fast neutron sulfur activation by 10% because of increased backscatter.

The shielding is generally no more than a 20% effect and is not required in order to demonstrate broad agreement between the DS02 fluence calculations and measurements. However, including the shielding of the fluence in the anal-

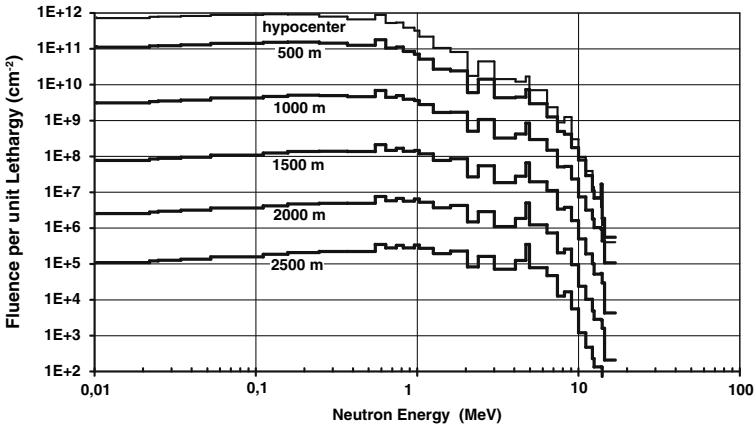

Fig. 1 Hiroshima DS02 neutron fluences as a function of energy at 1 m above ground for ground ranges of 0, 500, 1,000, 1,500, 2,000, and 2,500 m from the hypocenter

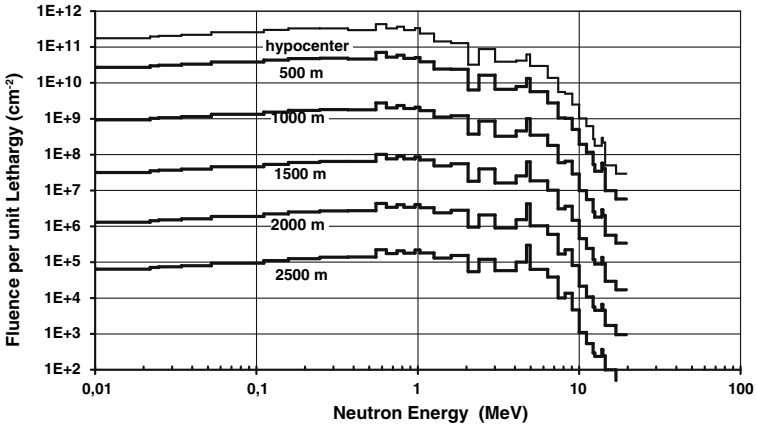

Fig. 2 Nagasaki DS02 neutron fluences as a function of energy at 1 m above ground for ground ranges of 0, 500, 1,000, 1,500, 2,000, and 2,500 m from the hypocenter

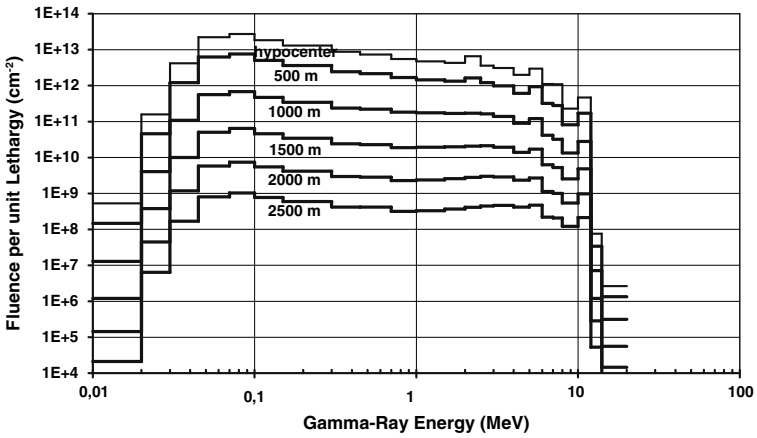

Fig. 3 Hiroshima DS02 gamma-ray fluences as a function of energy at 1 m above ground for ground ranges of 0, 500, 1,000, 1,500, 2,000, and 2,500 m from the hypocenter

ysis improves the agreement and strengthens the confidence in both the calculations and the measurements.

Conclusions

The DS02 FIA fluences are currently available from the 2002 calculations in the DABL69 energy group structure, and for the DS02 code in a DLC31 energy group structure. The 2002 calculation fluences from 0 to 2,500 m ground range are available as total fluence spectra or they can be partitioned according to the four radiation sources for which calculations were made. The DS02 code fluences are available as prompt and delayed fluences from 100 to 2,500 m ground range.

Both of these sets of fluences, at five heights for both cities, are also available in terms of angular distribution. The DS02 code fluences are currently being used at

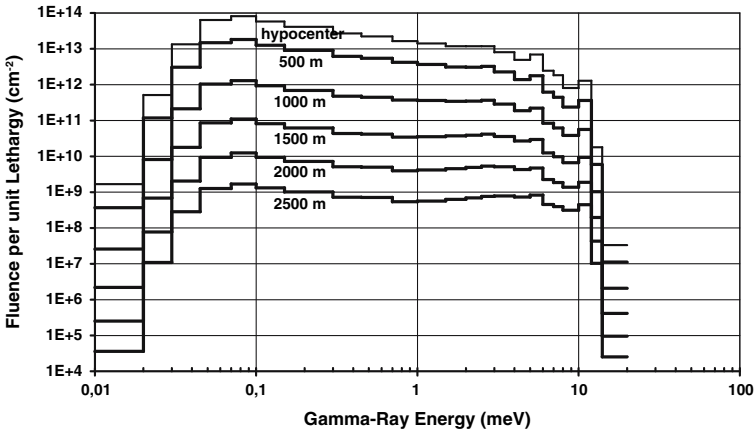

Fig. 4 Nagasaki DS02 gamma-ray fluences as a function of energy at 1 m above ground for ground ranges of 0, 500, 1,000, 1,500, 2,000, and 2,500 m from the hypocenter

Table 6 Energy group boundaries and fluence-to-kerma conversion coefficients used in the DS02 code

Group no.	Upper energy boundary (MeV)	Soft-tissue kerma coefficient (Gy cm^2)
Neutron		
1	$1.96 \times 10^{+1}$	6.73×10^{-11}
2	$1.69 \times 10^{+1}$	6.73×10^{-11}
3	$1.49 \times 10^{+1}$	6.61×10^{-11}
4	$1.42 \times 10^{+1}$	6.57×10^{-11}
5	$1.38 \times 10^{+1}$	6.47×10^{-11}
6	$1.28 \times 10^{+1}$	6.38×10^{-11}
7	$1.22 \times 10^{+1}$	6.33×10^{-11}
8	$1.11 \times 10^{+1}$	6.04×10^{-11}
9	$1.00 \times 10^{+1}$	5.83×10^{-11}
10	$9.05 \times 10^{+0}$	5.54×10^{-11}
11	$8.19 \times 10^{+0}$	5.45×10^{-11}
12	$7.41 \times 10^{+0}$	5.12×10^{-11}
13	$6.38 \times 10^{+0}$	4.71×10^{-11}
14	$4.97 \times 10^{+0}$	4.58×10^{-11}
15	$4.72 \times 10^{+0}$	4.43×10^{-11}
16	$4.07 \times 10^{+0}$	4.18×10^{-11}
17	$3.01 \times 10^{+0}$	3.55×10^{-11}
18	$2.39 \times 10^{+0}$	3.33×10^{-11}
19	$2.31 \times 10^{+0}$	3.20×10^{-11}
20	$1.83 \times 10^{+0}$	2.73×10^{-11}
21	$1.11 \times 10^{+0}$	2.02×10^{-11}
22	5.50×10^{-1}	1.30×10^{-11}
23	1.58×10^{-1}	8.06×10^{-12}
24	1.11×10^{-1}	5.64×10^{-12}
25	5.25×10^{-2}	3.17×10^{-12}
26	2.48×10^{-2}	2.14×10^{-12}
27	2.19×10^{-2}	1.49×10^{-12}
28	1.03×10^{-2}	6.39×10^{-13}
29	3.35×10^{-3}	2.21×10^{-13}
30	1.23×10^{-3}	9.25×10^{-14}
31	5.83×10^{-4}	3.09×10^{-14}
32	1.01×10^{-4}	1.04×10^{-14}
33	2.90×10^{-5}	9.37×10^{-15}
34	1.07×10^{-5}	1.36×10^{-14}
35	3.06×10^{-6}	2.28×10^{-14}
36	1.13×10^{-6}	3.74×10^{-14}
37	4.14×10^{-7}	1.50×10^{-13}
	1.00×10^{-11}	
Gamma ray		
38	$1.40 \times 10^{+1}$	2.66×10^{-11}
39	$8.94 \times 10^{+0}$	2.28×10^{-11}
40	$7.48 \times 10^{+0}$	1.98×10^{-11}
41	$7.00 \times 10^{+0}$	1.78×10^{-11}
42	$6.00 \times 10^{+0}$	1.61×10^{-11}
43	$5.00 \times 10^{+0}$	1.43×10^{-11}
44	$4.00 \times 10^{+0}$	1.21×10^{-11}
45	$3.00 \times 10^{+0}$	1.03×10^{-11}
46	$2.50 \times 10^{+0}$	8.96×10^{-12}
47	$2.00 \times 10^{+0}$	7.53×10^{-12}
48	$1.50 \times 10^{+0}$	5.84×10^{-12}
49	$1.00 \times 10^{+0}$	4.25×10^{-12}
50	7.00×10^{-1}	2.86×10^{-12}
51	4.50×10^{-1}	1.92×10^{-12}
52	3.00×10^{-1}	1.03×10^{-12}
53	1.50×10^{-1}	5.30×10^{-13}
54	1.00×10^{-1}	3.49×10^{-13}
55	7.00×10^{-2}	3.16×10^{-13}
56	4.50×10^{-2}	4.64×10^{-13}
57	3.00×10^{-2}	1.07×10^{-12}
58	2.00×10^{-2}	3.51×10^{-12}
	1.00×10^{-2}	

Table 7 Hiroshima DS02 code prompt and delayed components for neutron and gamma-ray FIA fluence at 1 m above ground for a ground range of 1,500 m

Group no.	Prompt (cm^{-2})	Delayed (cm^{-2})
Neutron		
1	$0.00 \times 10^{+0}$	
2	$6.56 \times 10^{+2}$	
3	$1.04 \times 10^{+3}$	
4	$7.81 \times 10^{+2}$	
5	$5.14 \times 10^{+3}$	
6	$2.46 \times 10^{+3}$	
7	$1.80 \times 10^{+4}$	
8	$5.19 \times 10^{+4}$	
9	$1.60 \times 10^{+5}$	
10	$3.77 \times 10^{+5}$	
11	$3.39 \times 10^{+5}$	
12	$1.68 \times 10^{+6}$	
13	$4.88 \times 10^{+6}$	
14	$3.36 \times 10^{+6}$	
15	$4.13 \times 10^{+6}$	$1.03 \times 10^{+5}$
16	$5.48 \times 10^{+6}$	$6.10 \times 10^{+4}$
17	$1.24 \times 10^{+7}$	$3.04 \times 10^{+5}$
18	$4.00 \times 10^{+6}$	$1.36 \times 10^{+5}$
19	$2.01 \times 10^{+7}$	$6.83 \times 10^{+5}$
20	$4.10 \times 10^{+7}$	$1.60 \times 10^{+6}$
21	$9.71 \times 10^{+7}$	$5.53 \times 10^{+6}$
22	$1.61 \times 10^{+8}$	$1.11 \times 10^{+7}$
23	$4.07 \times 10^{+7}$	$2.96 \times 10^{+6}$
24	$7.59 \times 10^{+7}$	$5.55 \times 10^{+6}$
25	$6.44 \times 10^{+7}$	$4.74 \times 10^{+6}$
26	$9.83 \times 10^{+6}$	$7.30 \times 10^{+5}$
27	$5.41 \times 10^{+7}$	$4.01 \times 10^{+6}$
28	$8.12 \times 10^{+7}$	$6.04 \times 10^{+6}$
29	$7.14 \times 10^{+7}$	$5.32 \times 10^{+6}$
30	$5.45 \times 10^{+7}$	$4.07 \times 10^{+6}$
31	$1.33 \times 10^{+8}$	$9.98 \times 10^{+6}$
32	$9.99 \times 10^{+7}$	$7.56 \times 10^{+6}$
33	$8.26 \times 10^{+7}$	$6.28 \times 10^{+6}$
34	$1.06 \times 10^{+8}$	$8.02 \times 10^{+6}$
35	$8.75 \times 10^{+7}$	$6.55 \times 10^{+6}$
36	$9.16 \times 10^{+7}$	$6.76 \times 10^{+6}$
37	$6.79 \times 10^{+8}$	$5.23 \times 10^{+7}$
Total	$2.09 \times 10^{+9}$	$1.50 \times 10^{+8}$
Gamma ray		
38	$8.63 \times 10^{+8}$	$2.16 \times 10^{+7}$
39	$5.42 \times 10^{+8}$	$2.62 \times 10^{+7}$
40	$6.35 \times 10^{+8}$	$6.97 \times 10^{+7}$
41	$8.43 \times 10^{+8}$	$1.27 \times 10^{+8}$
42	$2.36 \times 10^{+9}$	$7.37 \times 10^{+8}$
43	$1.53 \times 10^{+9}$	$1.58 \times 10^{+9}$
44	$1.81 \times 10^{+9}$	$3.78 \times 10^{+9}$
45	$9.32 \times 10^{+8}$	$2.95 \times 10^{+9}$
46	$1.13 \times 10^{+9}$	$3.47 \times 10^{+9}$
47	$1.32 \times 10^{+9}$	$4.40 \times 10^{+9}$
48	$1.72 \times 10^{+9}$	$6.09 \times 10^{+9}$
49	$1.49 \times 10^{+9}$	$5.24 \times 10^{+9}$
50	$2.72 \times 10^{+9}$	$7.33 \times 10^{+9}$
51	$2.47 \times 10^{+9}$	$7.25 \times 10^{+9}$
52	$5.76 \times 10^{+9}$	$1.80 \times 10^{+10}$
53	$4.52 \times 10^{+9}$	$1.40 \times 10^{+10}$
54	$4.91 \times 10^{+9}$	$1.79 \times 10^{+10}$
55	$4.72 \times 10^{+9}$	$1.77 \times 10^{+10}$
56	$1.20 \times 10^{+9}$	$2.84 \times 10^{+9}$
57	$4.64 \times 10^{+7}$	$1.07 \times 10^{+8}$
58	$2.83 \times 10^{+5}$	$5.48 \times 10^{+5}$
Total	$4.15 \times 10^{+10}$	$1.14 \times 10^{+11}$

Table 8 Nagasaki DS02 code prompt and delayed components for neutron and gamma-ray FIA fluence at 1 m above ground for a ground range of 1,500 m

Group no.	Prompt (cm^{-2})	Delayed (cm^{-2})
Neutron		
1	$2.52 \times 10^{+3}$	
2	$4.47 \times 10^{+3}$	
3	$3.17 \times 10^{+3}$	
4	$1.96 \times 10^{+3}$	
5	$8.73 \times 10^{+3}$	
6	$2.88 \times 10^{+3}$	
7	$2.28 \times 10^{+4}$	
8	$4.74 \times 10^{+4}$	
9	$1.46 \times 10^{+5}$	
10	$3.62 \times 10^{+5}$	
11	$3.07 \times 10^{+5}$	
12	$1.50 \times 10^{+6}$	
13	$4.54 \times 10^{+6}$	
14	$3.15 \times 10^{+6}$	
15	$3.68 \times 10^{+6}$	$2.60 \times 10^{+5}$
16	$4.69 \times 10^{+6}$	$1.46 \times 10^{+5}$
17	$8.57 \times 10^{+6}$	$5.72 \times 10^{+5}$
18	$2.52 \times 10^{+6}$	$2.29 \times 10^{+5}$
19	$1.22 \times 10^{+7}$	$1.14 \times 10^{+6}$
20	$2.36 \times 10^{+7}$	$2.54 \times 10^{+6}$
21	$4.54 \times 10^{+7}$	$8.07 \times 10^{+6}$
22	$6.30 \times 10^{+7}$	$1.54 \times 10^{+7}$
23	$1.48 \times 10^{+7}$	$4.05 \times 10^{+6}$
24	$2.67 \times 10^{+7}$	$7.60 \times 10^{+6}$

Table 8 continued

Group no.	Prompt (cm^{-2})	Delayed (cm^{-2})
25	$2.21 \times 10^{+7}$	$6.48 \times 10^{+6}$
26	$3.38 \times 10^{+6}$	$9.98 \times 10^{+5}$
27	$1.85 \times 10^{+7}$	$5.49 \times 10^{+6}$
28	$2.74 \times 10^{+7}$	$8.24 \times 10^{+6}$
29	$2.34 \times 10^{+7}$	$7.19 \times 10^{+6}$
30	$1.77 \times 10^{+7}$	$5.51 \times 10^{+6}$
31	$4.22 \times 10^{+7}$	$1.35 \times 10^{+7}$
32	$3.08 \times 10^{+7}$	$1.02 \times 10^{+7}$
33	$2.49 \times 10^{+7}$	$8.47 \times 10^{+6}$
34	$3.17 \times 10^{+7}$	$1.08 \times 10^{+7}$
35	$2.60 \times 10^{+7}$	$8.81 \times 10^{+6}$
36	$2.69 \times 10^{+7}$	$9.10 \times 10^{+6}$
37	$2.09 \times 10^{+8}$	$7.14 \times 10^{+7}$
Total	$7.19 \times 10^{+8}$	$2.06 \times 10^{+8}$
Gamma ray		
38	$1.70 \times 10^{+9}$	$2.47 \times 10^{+7}$
39	$1.47 \times 10^{+9}$	$2.67 \times 10^{+7}$
40	$1.21 \times 10^{+9}$	$8.27 \times 10^{+7}$
41	$1.78 \times 10^{+9}$	$1.49 \times 10^{+8}$
42	$4.49 \times 10^{+9}$	$8.73 \times 10^{+8}$
43	$4.09 \times 10^{+9}$	$1.88 \times 10^{+9}$
44	$4.88 \times 10^{+9}$	$5.40 \times 10^{+9}$
45	$3.01 \times 10^{+9}$	$4.53 \times 10^{+9}$
46	$3.33 \times 10^{+9}$	$5.29 \times 10^{+9}$
47	$3.93 \times 10^{+9}$	$6.70 \times 10^{+9}$
48	$5.16 \times 10^{+9}$	$9.20 \times 10^{+9}$
49	$4.43 \times 10^{+9}$	$7.88 \times 10^{+9}$
50	$7.41 \times 10^{+9}$	$1.09 \times 10^{+10}$
51	$6.86 \times 10^{+9}$	$1.08 \times 10^{+10}$
52	$1.60 \times 10^{+10}$	$2.68 \times 10^{+10}$
53	$1.26 \times 10^{+10}$	$2.06 \times 10^{+10}$
54	$1.34 \times 10^{+10}$	$2.59 \times 10^{+10}$
55	$1.28 \times 10^{+10}$	$2.48 \times 10^{+10}$
56	$3.29 \times 10^{+9}$	$3.93 \times 10^{+9}$
57	$1.29 \times 10^{+8}$	$1.47 \times 10^{+8}$
58	$7.65 \times 10^{+5}$	$7.42 \times 10^{+5}$
Total	$1.12 \times 10^{+11}$	$1.66 \times 10^{+11}$

RERF to calculate FIA kerma to soft tissue and absorbed doses to 15 organs of the body for individual survivors in the major RERF population study samples. A companion paper is planned that will provide typical DS02 fluence spectra (1) inside Japanese wooden houses, (2) behind dense shielding structures, and (3) within survivors' organs from the atomic-bomb at Hiroshima and Nagasaki.

Table 9 Effect of interface scattering materials relative to wet ground

Nuclear reaction	Ratios for nuclear reaction at 1 m above various interface materials to that at 1 m above standard DS02 wet ground containing 30% moisture			
	Damp ground (15% moisture)	Dry ground (no moisture)	Concrete	Granite
$^{35}Cl(n,\gamma)^{36}Cl$	0.96	0.81	0.83	0.69
$^{151}Eu(n,\gamma)^{152}Eu$	0.97	0.85	0.87	0.74
$^{59}Co(n,\gamma)^{60}Co$	0.98	0.90	0.92	0.85
Neutron kerma	1.06	1.25	1.25	1.43
$^{63}Cu(n,p)^{63}Ni$	1.04	1.09	1.09	1.16
$^{32}S(n,p)^{32}P$	1.04	1.09	1.09	1.15

Calculations for ^{41}Ca, ^{154}Eu and ^{39}Ar were not performed for this study. By comparing the ratio of the thermal cross section to epithermal resonance integral, it is found that $^{40}Ca(n,\gamma)^{41}Ca$ (ratio = 1.9) and $^{153}Eu(n,\gamma)^{154}Eu$ (ratio = 0.2) should behave like $^{35}Cl(n,\gamma)^{36}Cl$ (ratio = 2.4) and $^{59}Co(n,\gamma)^{60}Co$ (ratio = 0.5), respectively. On the other hand the fast neutron reaction, $^{39}K(n,p)^{39}Ar$, should behave like the fast reactions from the above table

Acknowledgments The DS02 report represents over 5 years of work by 20 members of a Joint Working Group established in the fall of 2000 by the US and Japanese government agencies responsible for the Radiation Effects Research Foundation (RERF). The Japanese members were appointed by the Japanese Ministry of Health, Labour and Welfare (MHLW) and the US members of US Department of Energy (DOE). The Joint Working Group, chaired by Dr. Robert W. Young and Dr. Hiromi Hasai, included an additional sixty contributing associated members from universities in the US, Japan, and Germany. The new DS02 was approved for use by RERF in March 2003 after an extensive review by eight members of a Joint Senior Review Committee, chaired by Dr. Warren Sinclair and Dr. Wataru Mori. A copy of the complete DS02 report is available on the RERF website at http://www.rerf.or.jp/shared/ds02/index.html. The RERF, Hiroshima and Nagasaki, Japan, is a private, non-profit foundation funded by the Japanese Ministry of Health, Labour, and Welfare and the US Department of Energy, the latter through the National Academy of Sciences. The material discussed in this report is taken mainly from work of the three authors and from sections of the DS02 report for which one of the three authors of this paper was the first author. One exception was Chap. 3 on Radiation Transport Calculations for Hiroshima and Nagasaki. The first author of this chapter was Mr. Robert T. Santoro who died during the final preparation of the DS02 Report. Following Mr. Santoro's death, the chapter was completed by two coauthors of Chap. 3 (Egbert and Kerr) with the help of Dr. John M. Barnes and Dr. Jeffery O. Johnson of the Oak Ridge National Laboratory. The work of government program managers (Dr. Joseph F. Weiss, DOE Office of Environment, Safety, and Health; Dr. David G. Thomassen, DOE Office of Science; and Drs. Hirotsugu Kimura, Shigeki Shiba, and Masami Kato, Health Service Bureau, MHLW) in facilitating funding for specific projects and the overall DS02 effort is also gratefully acknowledged.

References

1. Young RW, Kerr GD (ed) (2005) Reassessment of the atomic bomb radiation dosimetry for Hiroshima and Nagasaki—Dosimetry

System 2002 (DS02), vol 1, 2. Radiation Effects Research Foundation, Hiroshima, Japan
2. Kerr GD, Pace JV III, Mendelsohn E, Loewe WE, Kaul DC, Dolatshahi F, Egbert SD, Gritzner M, Scott WH Jr, Marcum J, Kosako T, Kanda K (1987) Transport of initial radiations in air over ground. In: Roesch WC (ed) US–Japan joint reassessment of atomic bomb radiation dosimetry in Hiroshima and Nagasaki, final report, vol 1. Radiation Effects Research Foundation, Hiroshima, Japan, pp 66–142
3. National Nuclear Data Center (2007) Chart of nuclides. At http://www.nndc.bnl.gov/chart, NNDC. Brookhaven National Laboratory, Brookhaven, New York
4. Rühm W, Kellerer AM, Korschinek G, Faestermann T, Knie K, Rugel G, Kato K, Nolte E (1998) The dosimetry system DS86 and the neutron discrepancy in Hiroshima—historical review, present status, and future options. Radiat Environ Biophys 37(4):293–310
5. Nagashima Y, Seki R, Matsuhiro T, Takahashi T, Sasa K, Sueki K, Hoshi M, Fujita S, Shizuma K, Hasai H (2004) Chlorine-36 in granite samples from the Hiroshima A-bomb site. Nucl Instr Meth Phys Res B 223–224:782–787
6. Straume T, Marchetti AA, Egbert SD, Roberts JA, Men P, Fujita S, Shizuma K, Hoshi M (2005) ^{36}Cl measurements in the United States Chap. 8 Part D. In: Young RW, Kerr GD (eds) Reassessment of the atomic bomb radiation dosimetry for Hiroshima and Nagasaki—Dosimetry System 2002 (DS02), vol 2. Radiation Effects Research Foundation, Hiroshima
7. Huber T, Rühm W, Hoshi M, Egbert SD, Nolte E (2003) ^{36}Cl measurements in Hiroshima granite samples as part of an international intercomparison study. Results from the Munich group. Radiat Environ Biophys 42:27–32
8. Huber T, Rühm W, Kato K, Egbert SD, Kubo F, Lazarev V, Nolte E (2005) The Hiroshima thermal neutron discrepancy for ^{36}Cl at large distances. Part I: new ^{36}Cl measurements in granite samples exposed to A-bomb neutrons. Radiat Environ Biophys 44:75–86
9. Shizuma K, Iwatani K, Hasai H, Hoshi M, Oka T (1997) ^{152}Eu depth profiles in granite and concrete cores exposed to the Hiroshima atomic bomb. Health Phys 76:848–855
10. Nakanishi T, Miwa K, Ohki R (1998) Specific radioactivity of europium-152 in roof tiles exposed to atomic bomb radiation in Nagasaki. J Radiat Res 39:243–250
11. Komura K, Hoshi M, Endo S, Imanaka T, Fukushima H (2005) Ultra-low-background measurements of ^{152}Eu in Hiroshima samples, Chap. 8 Part I. In: Young RW, Kerr GD (eds) Reassessment of the atomic bomb radiation dosimetry for Hiroshima and Nagasaki—Dosimetry System 2002 (DS02), vol 2. Radiation Effects Research Foundation, Hiroshima
12. Marchetti AA, Hainsworth LJ, McAninch JE, Leivers MR, Jones P, Straume T, Proctor ID (1997) Ultra-separation of nickel from copper metal for the measurement of ^{63}Ni by AMS. Nucl Instr Meth Phys Res B 123:230–234
13. Rühm W, Knie K, Rugel G, Marchetti AA, Faestermann T, Wallner C, McAninch JE, Straume T, Korschinek G (2000) Accelerator mass spectrometry of ^{63}Ni at the Munich Tandem Laboratory for estimating fast neutron fluences from the Hiroshima atomic bomb. Health Phys 79(4):358–364
14. Straume T, Rugel, G Marchetti AA, Rühm W, Korschinek G, McAninch JE, Carroll K, Egbert S, Faestermann T, Knie K, Martinelli R, Wallner A, Wallner C (2003) Measuring fast neutrons in Hiroshima at distances relevant to atomic-bomb survivors. Nature 424:539–542
15. Nolte E, Rühm W, Loosli HH, Tolstikhin I, Kato K, Huber TC, Egbert SD (2006) Measurements of fast neutrons in Hiroshima by use of ^{39}Ar. Radiat Environ Biophys 44:261–271
16. Ingersoll DT, White JE, Wright RQ, Hunter HT, Slater CO, Greene NM, Roussin RW, MacFarland RE (1995) Production and testing of the VITAMIN-B6 fine group and the BUGLE-93 broad group neutron/photon cross-section libraries derived from ENDF/B-VI nuclear data. NUREG/CR-6214, ORNL-6759. Oak Ridge National Laboratory, Oak Ridge, Tennessee
17. Ingersoll DT, Roussin RW, Fu CY, White JE (1989) DABL69: a broad-group neutron/photon cross-section library for Defense Nuclear Applications. ORNL/TM-10568, Oak Ridge National Laboratory, Oak Ridge, Tennessee
18. Roesch WC (ed) (1987) US-Japan joint reassessment of atomic bomb radiation dosimetry in Hiroshima and Nagasaki, final report, vols 1, 2. Radiation Effects Research Foundation, Hiroshima, Japan
19. Roesch WC, Attix FH (1968) Basic concepts in radiation dosimetry. In: Attix FH, Roesch WC, Tochilin E (eds) Radiation dosimetry, vol 1. Academic, New York, pp 1–92
20. International Commission on Radiological Protection (1975) Report of task group on Reference Man, ICRU Publication 23. Pergamon Press, Oxford, England
21. Kerr GD (1982) Photon and neutron fluence-to-kerma factors for ICRP-1975 Reference Man using improved elemental compositions for bone and marrow of the skeleton. ORNL/TM-8318, Oak Ridge National Laboratory, Oak Ridge, Tennessee
22. Hubbell JH, Seltzer SM (1996) Tables of X-ray mass attenuation and energy-absorption coefficients from 1 keV to 20 MeV for elements Z = 1 to 92 and 48 additional substances of dosimetric interest. NIST 5632, National Institute for Science and Technology, Gaithersburg, Maryland
23. International Commission on Radiation Units and Measurements (2000) Nuclear data for neutron and proton radiotherapy and for radiation protection, ICRU Report 63. ICRU Publications, Bethesda, Maryland
24. Bartine DE, Knight JR, Pace JV III, Roussin RW (1977) Production and testing of the DNA few-group coupled neutron-gamma cross-section library. ORNL/TM-4840 Oak Ridge National Laboratory, Oak Ridge, Tennessee
25. Briesmeister JF (1997) MCNP—a general Monte Carlo n-particle transport code, version 4B. LA-12625 Los Alamos National Laboratory, Los Alamos, New Mexico
26. Woolson WA, Gritzner ML, Egbert SD (1989) DS86 software description. Science Applications International Corporation, La Jolla, California